Prediction of Redox Potentials for Different Oxidation States of U, Np, Pu, and Am in Alkaline Aqueous Solution

Felipe R. Dutra and David A. Dixon*

Cite This: *J. Phys. Chem. A* 2025, 129, 2521−2536

ABSTRACT: The redox potentials for U, Np, Pu, and Am for oxidation states +III up to +VIII in alkaline aqueous solutions were predicted using density functional theory (DFT) and small-core pseudopotentials and their basis sets, with a hybrid explicit/implicit solvent model using SHE = 4.28 V. For each oxidation state, various oxo/hydroxo complexes were evaluated, resulting in a variety of one-electron redox pathways. For An(VIII/VII) couples, the predicted redox potentials for the $[An(VIII)O_5(OH)]^{-3}$/ $[An(VII)O_4(OH)_2]^{-3}$ or $[An(VIII)O_4(OH)_2]^{-2}$/$[An(VII)O_4(OH)_2]^{-3}$ couples are in good agreement with existing estimates. For An(VII/VI) redox couples, all couples, particularly $[An(VII)O_4(OH)_2]^{-3}$/ $[An(VI)O_2(OH)_4]^{-2}$, were in agreement with experimental values for U, Np, and Pu, but the results for Am showed larger differences from the estimated potentials. The An(VI/V) couples were consistent with experiments for dioxo/tetrahydroxo couples, and the An(V/IV) couples showed acceptable agreement based on actinide-specific couples, with neutral hydroxides often favored in the +IV state. The An(IV/III) couples were consistent with the literature values when modeled as soluble neutral hydroxides. The use of our approach yielded calculated redox potentials that were within ±0.2 V of experimental or estimated values consistent with our prior calculations on redox potentials of actinides from Ac to Am in acidic aqueous solutions. This supports the robustness of our DFT-based methodology for predicting actinide redox potentials, offering valuable insights into actinide chemistry in aqueous solutions.

INTRODUCTION

The actinides play an important role in nuclear energy generation as well as in the production of nuclear weapons. The use of these materials has generated significant quantities of radioactive waste, necessitating appropriate treatment and management.[1] These wastes contain compounds of U, Np, Pu, and Am, in different phases and oxidation states depending on the pH of the aqueous solution.[2] Understanding the chemistry of these actinides is essential for their reprocessing, storage, and environmental remediation.[3,4] The behavior of actinides under alkaline to hyperalkaline conditions remains an area of significant interest.[5] Under such conditions, wastes tend to form hydroxides with low solubility, resulting in the formation of sludges and solids in a slurry phase.[6] The presence of these materials in waste tanks such as those at the Hanford site in Washington state in the USA poses a significant threat to the surrounding environment, as possible leaks could contaminate the nearby soil or underground water sources.[7,8] It is important to note that many of the waste storage tanks at the Hanford site are highly alkaline due to the addition of base to quench the acidic conditions under which the actinides were processed.

In alkaline media, actinide compounds have been reported to exhibit oxidation states ranging from +VII to +III.[9] The highest oxidation states, +VII, +VI, and +V, are more stable in alkaline media than in acidic media due to the availability of OH^- ligands that can stabilize the excess positive charge.[10] In contrast, the lower oxidation states, +III and + IV, exhibit greater instability in basic conditions and tend to form insoluble hydroxides.[11] Thus, the exact speciation is highly dependent on the hydroxide concentration in the solution.[12] The +VIII state has been claimed to be observed experimentally for Pu(VIII),[13−17] and some studies suggest the possible existence of Am(VIII).[18] However, other studies provide contradictory evidence for the existence of the +VIII oxidation state in aqueous solutions.[19−21]

Data on the redox potentials of actinide couples are required to predict speciation and reactions in a particular medium. Performing direct potential measurements is challenging due to the high ionic strength and formation of insoluble products in alkaline conditions as well as the radioactivity of the samples. Consequently, there are significant differences in the literature.[22] Estimates[9,14,23−31] and experimental redox data[12,30,32−39] for actinides in alkaline media are usually available only for a limited number of elements, generally in higher oxidation states. As such, it is useful to employ computational electronic structure methods to predict redox potentials. In our previous studies, we predicted reduction

potentials for actinides from Ac to Pu across multiple oxidation states in acidic media.[40,41] Our approach involves using thermodynamic cycles incorporating solvated ions within an extended solvation shell in conjunction with an implicit solvation model. In our approach[40,41] based on comparison to experiment, the spin−orbit corrections were found to approximately cancel within the error bars of these calculations. At the level of density functional theory (DFT) with the B3LYP functional, two explicit solvation shells, and the implicit COSMO solvent model, satisfactory predictions were achieved with differences from experimental values by less than 0.2 V in most cases. In the current work, we used this method to predict reduction potentials in alkaline aqueous environments for the elements U, Np, Pu, and Am in various oxidation states.

COMPUTATIONAL METHODS

The Gibbs free energy for the reduction half-cell reaction can be calculated by using thermodynamic cycles. We assume that the species in the gas phase and solution phase are at states of 1 atm and 1 mol/L, respectively. We adopted the ion convention for all cases. The full cell potentials related to the standard hydrogen electrode can be calculated using eq 1

$$E^{o} = -\frac{\Delta G_{soln}^{*}}{zF} + E^{o}_{SHE} \quad (1)$$

where ΔG^{*}_{soln} is the Gibbs free energy of the reduction halfcell reaction, z is the number of electrons transferred in the reaction, F is the Faraday constant, and E^{o}_{SHE} is the cell potential for the standard hydrogen electrode (SHE). The absolute value of the SHE adopted in this study is −4.28 V.[42] Depending on the redox couple, various half-reactions were explored. The equations used for calculating each cycle are given in the Supporting Information. The An(VIII/VII) reduction process is described by the cycles shown in Figure 1. The first two cycles (eqs 2 and 3) involve a direct electron

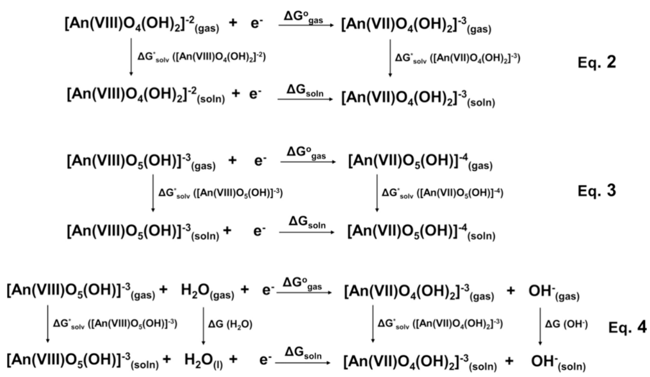

Figure 1. Thermodynamic cycles used for the predictions of the An(VIII/VII) reduction potentials.

transfer, without formation/breaking of bonds. In this case, the standard state corrections related to a change of the solute from a 1 atm gas state to a 1 mol/L aqueous state will cancel each other. The third cycle (eq 4) displays another possibility for the reaction, where the octavalent species exist as a pentaoxo/hydroxo complex and redox will involve breaking/ formation of bonds. This cycle contains water in the liquid phase, for which the concentration is $[H_2O]$ = 55.5 mol/L. The experimental Gibbs free energy of the change of H_2O(g, 1 atm) to H_2O(l, 55 mol/L) at 298.15 K corresponds to −2.05 kcal/mol.[43] The solvation energy for the hydroxide anion has been previously studied, and we adopt a value of −104.5 kcal/ mol.[44] However, since those values are determined using 1 mol/L in both phases, a correction term related to the change of 1 atm to 1 mol/L (1.89 kcal/mol) needs to be considered. Including these corrections, the OH^- solvation energy decreased by −102.6 kcal/mol. The remaining standard state corrections for the actinide species will cancel each other. The equations used for calculating the Gibbs free energy in solution are described in the Supporting Information.

The redox processes involving the An(VII/VI) couple were explored assuming multiple forms of An(VI) species as shown in Figure 2.

Since the exact speciation for the An(V) is not exactly known, a number of half-reactions for the An(VI/V) couple were evaluated, maintaining a coordination number (CN) of 6. The reactions used are given in Figures 3, 4, and 5, with eqs 8− 19 for each of the cycles.

Redox potentials for the An(V/IV) couple have been obtained experimentally.[37−39] These processes are influenced by the formation of solids with extremely low solubilities. However, some studies suggest the existence of ionic forms for the An(IV) species. In this work, the An(V/IV) redox potentials were calculated considering all possibilities for An(V) and assuming that An(IV) is present in the soluble form as $An(OH)_4(H_2O)_2$(aq) neutral hydroxide species or as the anions $An(IV)(OH)_5(H_2O)^{-1}$ or $An(IV)(OH)_6^{-2}$, all maintaining CN = 6. Figures 6, 7, 8, and 9 describe the redox process involving the An(V/IV), and eqs 20–31 describe the equations used to calculate ΔG^*_{soln} for each cycle.

The An(IV/III) redox couples were also calculated. The An(III) species exists preferably as insoluble hydroxides under 1 M NaOH conditions. Similarly, the An(IV/III) redox potentials were calculated assuming that An(III) is present in a soluble form as $An(OH)_3(H_2O)_2(aq)$ and all possibilities for An(IV) as shown in Figure 10, eqs 32–34.

To account for explicit solvent effects, the anionic actinide complexes were solvated with 30 H_2O molecules using the supermolecule-continuum approach. The solvation energies were calculated using two implicit solvent models, COSMO[45,46] and SMD.[47] Clark and co-workers[48] demonstrated that clusters containing this number of solvent molecules, including a second solvation shell, effectively minimized errors in both the electrostatic and nonelectrostatic contributions to the solvation free energy.[48,49] Additionally, as demonstrated in our prior work,[40,41] this number of solvent molecules is appropriate for representing the solvation of the system in combination with an implicit self-consistent reaction field giving redox potentials to within ±0.2 V in most cases. The geometries for the clusters in this work were optimized at the density functional theory (DFT)[50] level with the B3LYP[51,52] and PW91[53] functionals (the latter only for Pu complexes based on our previous work[40,41]) using the Gaussian16 program.[54] All calculations were performed by using the quadratically convergent (XQC) algorithm to avoid convergence problems in the SCF calculations. The Stuttgart small-core relativistic effective core potential (60ECP) with the accompanying segmented basis set was used for the actinide atoms.[55–58] The TZVP basis set was used for O and H with diffuse s and p added to O based on a geometric extrapolation of the outer exponents to better treat the anions. The vibrational frequencies were adjusted using the GoodVibes

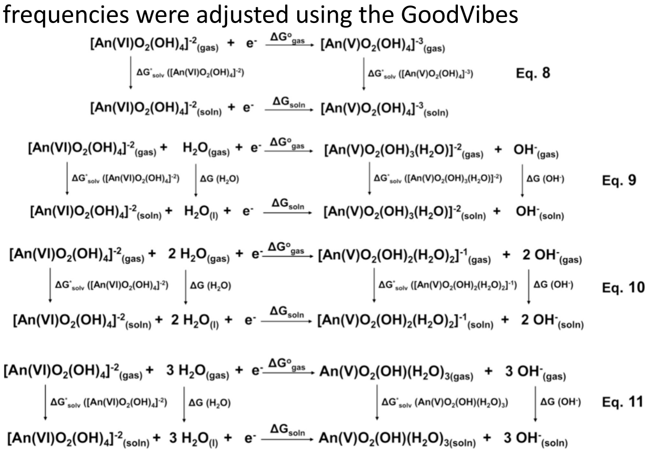

Figure 3. Thermodynamic cycles used for the predictions of An(VI/V) reduction potentials, with An(VI) = $[An(VI)O_2(OH)_4]^{-2}$.

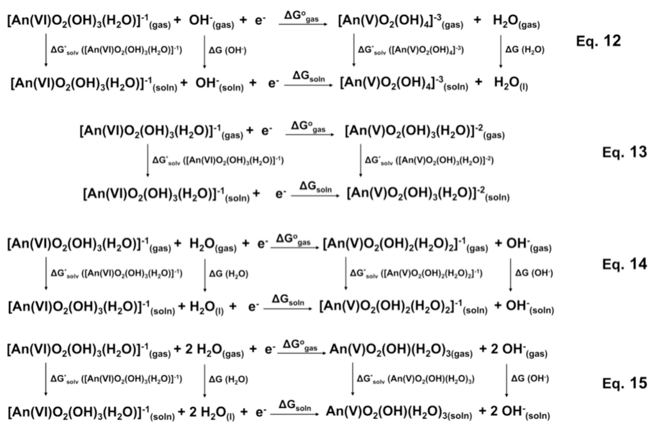

Figure 4. Thermodynamic cycles used for the predictions of An(VI/V) reduction potentials, with An(VI) = $[An(VI)O_2(OH)_3(H_2O)]^{-1}$.

program,[59] which applies a scaling factor to account for anharmonicity, depending on the level of theory/basis set used, and adjusts vibrational modes lower than 100 cm^{-1} to 100 cm^{-1} following Truhlar and co-workers.[60] This approximation is necessary, as the large numbers of solvent molecules can result in many low-frequency vibrational modes, which significantly impact entropy calculations under the harmonic approximation. As demonstrated in our previous studies,[40,41] our current method is capable of predicting redox potentials to within ±0.2 V.

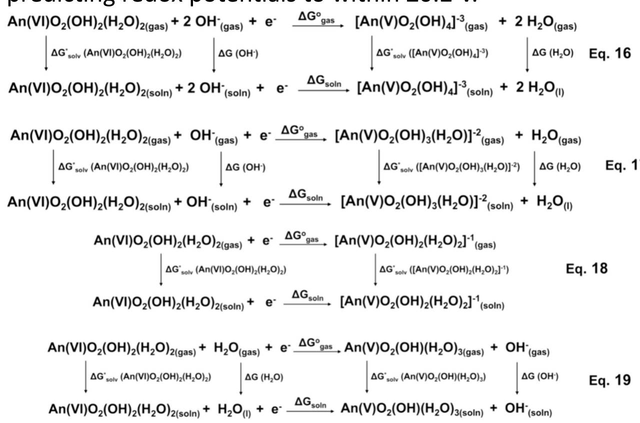

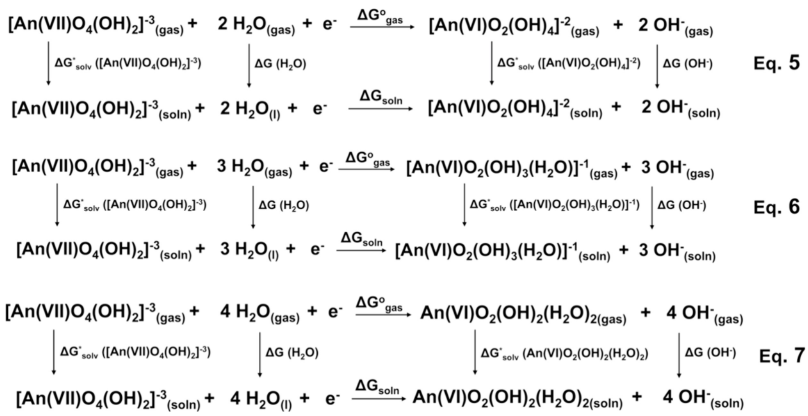

Figure 2. Thermodynamic cycle used for the predictions of An(VII/VI) reducti on potentials.

Figure 5. Thermodynamic cycles used for the predictions of An(VI/V) reduction potentials, with An(VI) = $An(VI)O_2(OH)_2(H_2O)_2$.

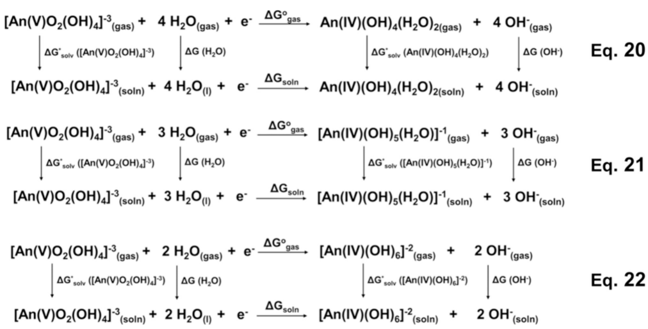

Figure 6. Thermodynamic cycles used for the predictions of An(V/IV) reduction potentials, with An(V) = $[An(V)O_2(OH)_4]^{-3}$.

Although we are fully optimizing the structures to find the lowest-energy geometry in these species without symmetry, we are certainly not completely sampling all the configuration space for these systems, which is a very large computational task with these many loosely bound water molecules. An approach to the sampling issue in the prediction of redox potentials in aqueous solution is to use ab initio molecular dynamics based on density functional theory in combination with free energy perturbation theory using thermodynamic integration to predict the free energy of insertion of an electron, equivalently the work function.[61,62] In this approach, the electron insertion process for the proton is calculated as well to serve as the SHE reference state, which leads to cancellation of errors. The use of nonhybrid DFT exchange−

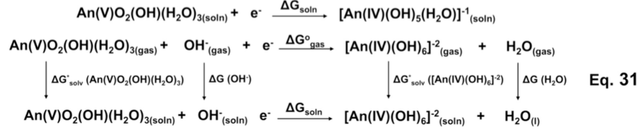

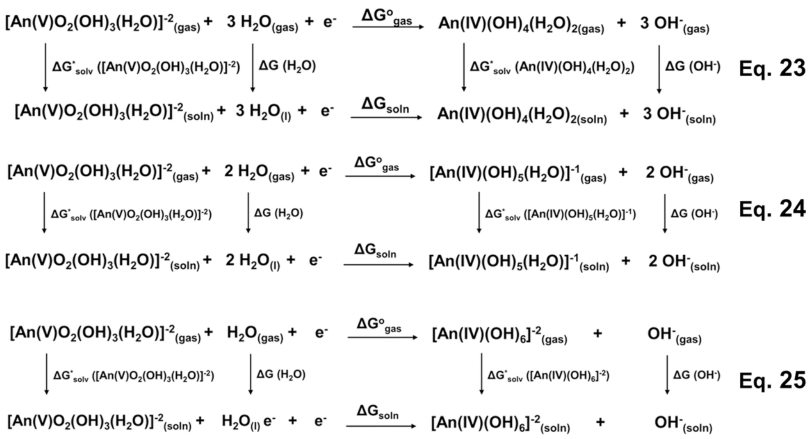

Figure 7. Thermodynamic cycles used for the predictions of An(V/IV) reduction potentials, with An(V) = $[An(V)O_2(OH)_3(H_2O)]^{-2}$.

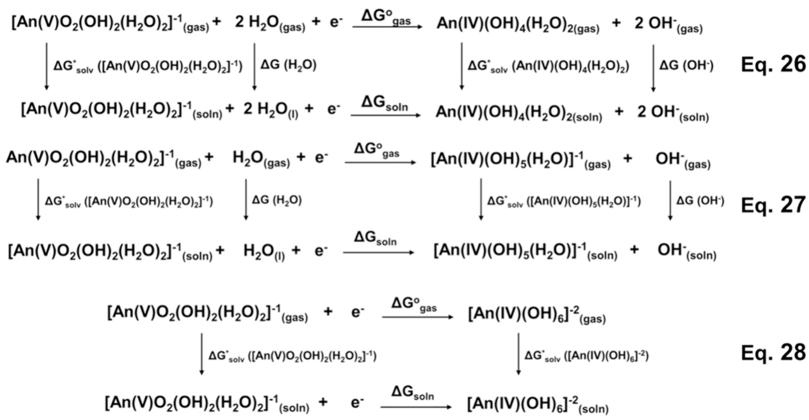

Figure 8. Thermodynamic cycles used for the predictions of An(V/IV) reduction potentials, with An(V) = $[An(V)O_2(OH)_2(H_2O)_2]^{-1}$.

Figure 9. Thermodynamic cycles used for the predictions of An(V/IV) reduction potentials, with An(V) = $An(V)O_2(OH)(H_2O)_3$.

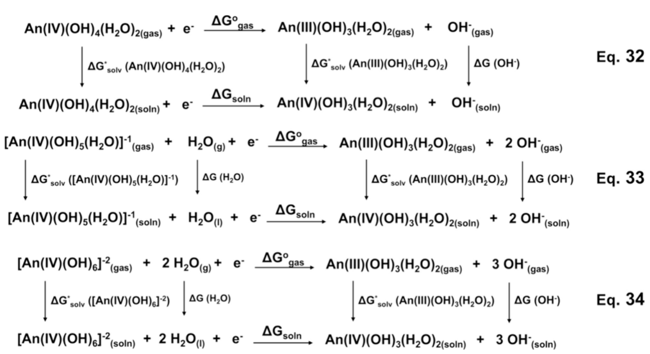

Figure 10. Thermodynamic cycles used for the predictions of the An(IV/III) reduction potentials.

correlation functionals[61] leads to errors in the predicted redox values due to issues with bandgap predictions due to delocalization issues.[63] The use[61] of hybrid functionals with some amount of Hartree−Fock exchange gives errors on the order of ±0.2 V in the redox potential. This level of error is the same level of error as found in the current work and in our prior work in acidic media,[40,41] with the exception that we use an absolute value for the SHE potential from experiment rather than a computed one. We also note that the DFT/ thermodynamic integration approach has been noted to have issues[61] when the excited states of the solute approach the edges of the band gap in water which our approach does not have. We have used our approach with differing numbers of solvent molecules chosen for the specific problem for a wide range of redox potentials of cations and anions and have found excellent agreement with experiment within ±0.2 V and often significantly better.[40,41,64−67] Our approach is appropriate for systems of infinite dilution (ionic strength = 0) as no counterions are present in our simulations.

RESULTS AND DISCUSSION

Structural Parameters. Figures 11, 12, 13, and 14 illustrate the geometries of all of the species studied in this work. From +VIII to +IV, all structures assume the form of a distorted octahedron. The +III molecules resemble a distorted trigonal bipyramidal geometry. Experimental data for the actinides in alkaline solution are available only for a few species in the higher oxidation states, namely, for U(VI), Np(VII), and Np(VI). EXAFS and DFT studies are consistent in terms of

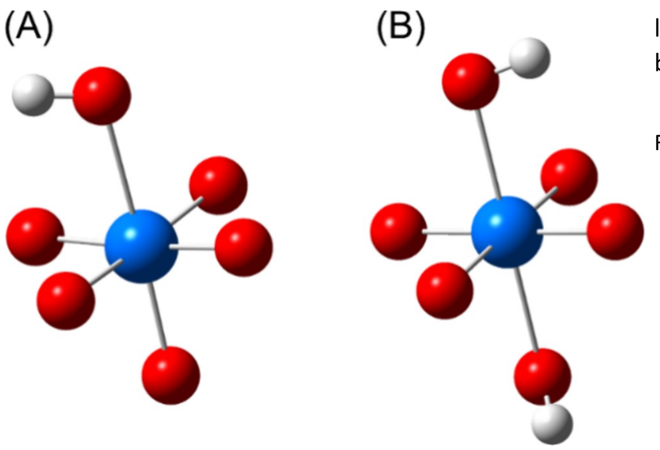

Figure 11. An(VIII) and An(VII) species. (A) $[AnO_5(OH)]^{-3/-4}$ and (B) $[AnO_4(OH)_2]^{-2/-3}$.

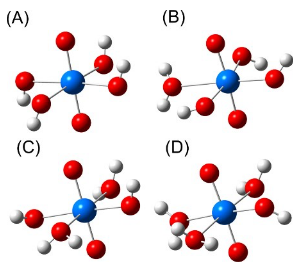

Figure 12. An(VI) and An(V) species. (A) $[AnO_2(OH)_4]^{-2/-3}$, (B) $[AnO_2(OH)_3(H_2O)]^{-1/-2}$, (C) $[AnO_2(OH)_2(H_2O)_2]^{0/-1}$, and (D) $AnO_2(OH)(H_2O)_3$.

the speciation and An–O bond distances.[68–70] Table 1 presents the parameters obtained in our study and the available experimental data in the literature. For the known structures, the calculated AnO bond distances are in good agreement with experiments within 0.04 Å.

Table 2 displays the bond lengths for the molecules in the current study. For the +VIII oxidation states of Pu and Am, the AnO bond lengths range from 1.84 to 1.97 Å. In the +VII oxidation state, the AnO bond lengths fall in a narrower range from 1.89 to 1.91 Å. For the +VI oxidation state, the AnO bond lengths are slightly shorter than those in the +VII oxidation state. For the +V oxidation state, the AnO bond lengths fall in a similar range of 1.83–1.94 Å. The actinyl An O bonds for the +VI and +V oxidation states of these

Figure 13. An(IV) species. (A) $An(OH)_4(H_2O)_2$, (B) $[An(OH)_5(H_2$

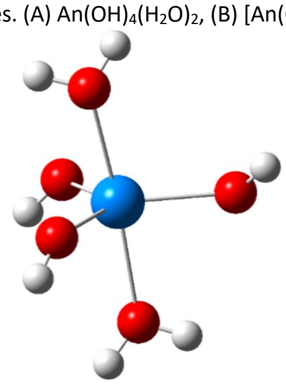

Figure 14. Neutral $An(III)(OH)_3(H_2O)_2$.

Table 1. Comparison between Averaged Experimental and Calculated Bond Lengths in Å for the Actinide Oxo/Hydroxo Complexes in Å Calculated at the B3LYP/ECP(60)/Modified-TZVP Level

cluster	spin	*R*(An– H) calc	*R*(An– H) expt	*R*(AnO) calc	*R*(AnO) expt
$[U(VI)O_2(OH)_4(H_2O)_{30}]^{-2}$,[a]	1	2.30	2.26[68]	1.82	1.82[68]
$[Np(VII)O_4(OH)_2(H_2O)_{30}]^{-3}$	1	2.38	2.24[69,70]	1.91	1.87[69,70]
$[Np(VI)O_2(OH)_4(H_2O)_{30}]^{-2}$ [a]	2	2.26	2.21[70]	1.83	1.82[70]

Determined in the tate. solid

complexes with OH^- in the equatorial plane are longer than the corresponding actinyl bonds calculated in acidic media with H_2O in the equatorial plane,[40] as the OH^- ligands weaken the AnO bond.

The An–OH bond lengths in the +VIII oxidation state vary from 2.27 to 2.40 Å. In the +VII oxidation state, these bond lengths fall in the range of 2.35–2.38 Å. For the +VI oxidation state, the An–OH bond lengths are shorter in the range of 2.20–2.28 Å across the actinides. In the +V state, the An–OH bond lengths fall in a range of 2.29–2.38 Å similar to the +VII

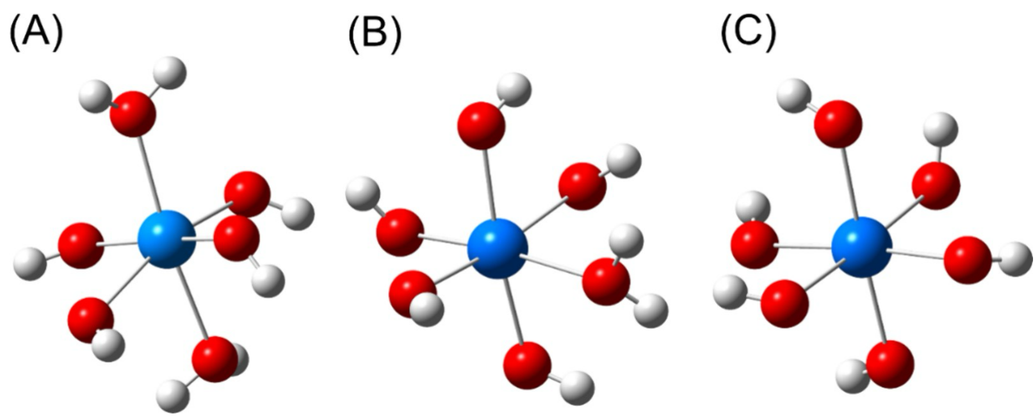

oxidation state. In the +IV state, the hydroxide bond lengths are in the same range of 2.17−2.29 Å as found for the +VI oxidation state. Finally, in the +III state, the An−OH bond lengths fall in a smaller range of 2.25−2.27 Å. Thus, the An− OH bond distances fall between ∼2.20 and 2.40 Å independent of the oxidation state.

O)]$^{-1}$, and (C) $[An(OH)_6]^{-2}$.

2. Calculated Average Bond Lengths (Å) for Various Actinides in Alkaline Media across Different Oxidation States at the B3LYP/ECP(60)/Modified-TZVP Level

species	bond type	U	Np	Pu	Am
VIII					
$[An(VIII)O_4(OH)_2(H_2O)_{30}]^{-2}$	AnO			1.84	1.84
	An−OH			2.27	2.27
$[An(VIII)O_5(OH)(H_2O)_{30}]^{-3}$	AnO			1.91	1.97
	An−OH			2.37	2.40
VII					
$[An(VII)O_4(OH)_2(H_2O)_{30}]^{-3}$	AnO		1.91	1.89	1.90
	An−OH		2.38	2.36	2.35
VI					
$[An(VI)O_2(OH)_4(H_2O)_{30}]^{-2}$	AnO	1.85	1.80	1.81	1.79
	An−OH	2.27	2.26	2.27	2.28
$[An(VI)O_2(OH)_3(H_2O)(H_2O)_{30}]^{-1}$	AnO	1.85	1.83	1.80	1.79
	An−OH	2.21	2.22	2.23	2.23
	An−O_{H2O}	2.46	2.44	2.45	2.46
$An(V)O_2(OH)_2(H_2O)_2(H_2O)_{30}$	AnO	1.82	1.79	1.77	1.75
	An−OH	2.20	2.20	2.21	2.22
	An−O_{H2O}	2.41	2.41	2.43	2.45
V					
$[An(V)O_2(OH)_4(H_2O)_{30}]^{-3}$	AnO	1.94	1.91	1.88	1.89
	An−OH	2.35	2.38	2.38	2.37
$[An(V)O_2(OH)_3(H_2O)(H_2O)_{30}]^{-2}$	AnO	1.94	1.92	1.89	1.91
	An−OH	2.31	2.31	2.32	2.29
	An−O_{H2O}	2.55	2.58	2.57	2.54
$[An(V)O_2(OH)_2(H_2O)_2(H_2O)_{30}]^{-1}$	AnO	1.90	1.87	1.85	1.86
	An−OH	2.30	2.32	2.32	2.31
	An−O_{H2O}	2.50	2.55	2.51	2.50
$An(V)O_2(OH)(H_2O)_3(H_2O)_{30}$	AnO	1.88	1.85	1.83	1.83
	An−OH	2.27	2.29	2.30	2.29
	An−O_{H2O}	2.49	2.50	2.50	2.49
IV					
$An(IV)(OH)_4(H_2O)_2(H_2O)_{30}$	An−OH	2.20	2.20	2.19	2.17
	An−O_{H2O}	2.50	2.45	2.43	2.48
$[An(IV)(OH)_5(H_2O)(H_2O)_{30}]^{-1}$	An−OH	2.24	2.24	2.23	2.21
	An−O_{H2O}	2.64	2.47	2.46	2.65
$[An(IV)(OH)_6(H_2O)_{30}]^{-2}$	An−OH	2.29	2.28	2.27	2.26
III					
$An(III)(OH)_3(H_2O)_2(H_2O)_{30}$	An−OH	2.27	2.27	2.25	2.25
	An−O_{H2O}	2.54	2.52	2.50	2.49

The An−OH_2 bond lengths are consistently longer than those of An−OH, across all oxidation states reflecting a weaker interaction with the actinide. For the +VI species, the distances varied between 2.41 and 2.46 Å. In the +V oxidation state, the bond lengths are generally longer (2.49−2.58 Å) highlighting weaker interactions. In the +IV state, the distances varied within a broader range of 2.43−2.65 Å, whereas for the +III state, it varied between 2.49 and 2.54 Å.

Reduction Potentials. Tables 3−7 present the redox potentials in aqueous alkaline solution for multiple actinide ions using the B3LYP functional. Table 8 presents the results using the PW91 functional for Pu redox couples. Experimental alkaline redox data[12,30,32−39] are available for some couples as well as a number of estimated values.[9,14,23−31] Most of the experimental data are obtained with [NaOH] = 1 M except for one Np(V/IV) result. As discussed above, the exact speciation of the actinides in alkaline media depends upon the $[OH^-]$ concentration. The stability region of water is important for an aqueous redox process. If such a process involves potentials within this stability region, then it can proceed in water without decomposing the water itself. Conversely, if the redox potential of the reaction falls outside this window, water will undergo electrolysis, producing hydrogen or oxygen gas, which can interfere with or prevent the determination of the desired redox process. The stability region varies with pH; at pH 14, the range extends from −0.829 to 0.401 V relative to SHE.

An(VIII/VII) Redox Potentials. It has long been speculated that the +VIII oxidation state is stable in highly concentrated alkaline solutions, particularly for Pu(VIII).[71] Experimental results have claimed that this state was achieved by ozonolysis of Pu oxo/hydroxo complexes in alkaline media.[13−15] However, a recent experimental study suggests that this oxidation state cannot be achieved under any conditions.[19] Computational studies indicate that PuO_4 as observed in gasphase experiments is actually a $(Pu(V)O_2)^+(O_2)^{-1}$ complex with Pu in the +V oxidation state.[72] This complex is significantly more stable than the proposed square-

3. An(VIII/VII) Potentials E^o for Actinides in Alkaline Aqueous Solution Calculated at the B3LYP/ECP(60)/ModifiedLevel[a]

An(ox)	An(red)	E^o COSMO	E^o SMD	E_{oest}
$[Pu(VIII)O_4(OH)_2(H_2O)_{30}]^{-2}$	$[Pu(VII)O_4(OH)_2(H_2O)_{30}]^{-3}$	1.94	1.93	≥1.15[23]
$[Pu(VIII)O_5(OH)(H_2O)_{30}]^{-3}$	$[Pu(VII)O_5(OH)(H_2O)_{30}]^{-4}$	1.47	1.53	
$[Pu(VIII)O_5(OH)(H_2O)_{30}]^{-3}$	$[Pu(VII)O_4(OH)_2(H_2O)_{30}]^{-3}$	2.58	2.57	
$[Am(VIII)O_4(OH)_2(H_2O)_{30}]^{-2}$	$[Am(VII)O_4(OH)_2(H_2O)_{30}]^{-3}$	1.55	1.61	≥1.6[24]
$[Am(VIII)O_5(OH)(H_2O)_{30}]^{-3}$	$[Am(VII)O_5(OH)(H_2O)_{30}]^{-4}$	0.65	0.84	
$[Am(VIII)O_5(OH)(H_2O)_{30}]^{-3}$	$[Am(VII)O_4(OH)_2(H_2O)_{30}]^{-3}$	1.63	1.62	

[a] Potentials in volts relative to SHE.

Table 4. An(VII/VI) Potentials E^o for Actinides in Alkaline Aqueous Solution Calculated at the B3LYP/ECP(60)/ModifiedTZVP Level[a]

An(ox)	An(red)	E^o COSMO	E^o SMD	E_{oest}	E_{oexp}
$[Np(VII)O_4(OH)_2(H_2O)_{30}]^{-3}$	$[Np(VI)O_2(OH)_4(H_2O)_{30}]^{-2}$	0.66	0.85		0.582[32]
$[Np(VII)O_4(OH)_2(H_2O)_{30}]^{-3}$	$[Np(VI)O_2(OH)_3(H_2O)(H_2O)_{30}]^{-1}$	0.64	0.88		
$[Np(VII)O_4(OH)_2(H_2O)_{30}]^{-3}$	$Np(VI)O_2(OH)_2(H_2O)_2(H_2O)_{30}$	0.57	0.90		
$[Pu(VII)O_4(OH)_2(H_2O)_{30}]^{-3}$	$[Pu(VI)O_2(OH)_4(H_2O)_{30}]^{-2}$	1.09	1.40	0.685[14]	0.849[33]
$[Pu(VII)O_4(OH)_2(H_2O)_{30}]^{-3}$	$[Pu(VI)O_2(OH)_3(H_2O)(H_2O)_{30}]^{-1}$	1.02	1.13		
$[Pu(VII)O_4(OH)_2(H_2O)_{30}]^{-3}$	$Pu(VI)O_2(OH)_2(H_2O)_2(H_2O)_{30}$	0.89	1.06		
$[Am(VII)O_4(OH)_2(H_2O)_{30}]^{-3}$	$[Am(VI)O_2(OH)_4(H_2O)_{30}]^{-2}$	1.88	2.04	1.05[25]	
$[Am(VII)O_4(OH)_2(H_2O)_{30}]^{-3}$	$[Am(VI)O_2(OH)_3(H_2O)(H_2O)_{30}]^{-1}$	1.82	2.04		
$[Am(VII)O_4(OH)_2(H_2O)_{30}]^{-3}$	$Am(VI)O_2(OH)_2(H_2O)_2(H_2O)_{30}$	1.71	2.02		

[a] Potentials in volts relative to SHE.

planar $Pu(VIII)O_4$ molecule.[73] Other studies suggest that Pu(VIII) may be, at most, metastable in oxyfluoride complexes highlighting the difficulty in reaching the octavalent oxidation state in Pu.[74]

The speciation of +VII species has been studied, and it is generally assumed that the heptavalent oxidation state prefers anions of the form $[An(VII)O_4(OH)_2]^{-3}$.[69,70,75] Tananaev et al.[76] suggested that, at [NaOH] = 10−18 M, Pu(VII) may assume the form of $[Pu(VII)O_5(OH)]^{-4}$ or $Pu(VII)O_6^{-5}$. Nevertheless, different estimates for the Pu(VIII/VII)[13,23] and Am(VIII/VII)[24] redox couples in alkaline media have been made. For all couples explored for Pu(VIII/VII), our calculations predicted positive potentials (Table 3). The most favorable reduction process for this couple is $[Pu(VIII)O_5OH]^{-3}/[Pu(VII)O_4(OH)_2]^{-3}$, which involves breaking and forming new bonds with a potential of ∼2.6 V. The couple consisting of pentaoxo/hydroxo complexes had predicted potentials of ∼1.5 V. However, it is very unlikely that the process occurs in $[OH^-]$ = 1 M, as there is experimental evidence indicating that the VII species exist predominantly as tetraoxo/dihydroxo complex anions, $[An(VII)O_4(OH)_2]^{-3}$.[20,69] The reduction potential of the $[Pu(VIII)O_4(OH)_2]^{-2}/[Pu(VII)O_4(OH)_2]^{-3}$ couple was predicted to have potentials of ∼1.9 V, a value significantly outside of the stability region of water at pH 14.

Tsushima[77] used computational methodologies to calculate the Pu(VIII/VII) redox process with different ligands. Tsushima used the B3LYP functional in combination with a Stuttgart ECP(60) for Pu and O atoms with the 6-311G(d,p) basis set for H; solvation effects were modeled with the implicit CPCM-UAHF model. However, no explicit solvation was considered for any of the anions. The spin−orbit effect of Pu(VII) species was calculated at the CASSCF level within the variation-perturbation scheme using the RASSI-SO[78] approach in MOLCAS.[79] Tsushima predicted potentials of 1.54 and 1.06 V for the $[Pu(VIII)O_4(OH)_2]^{-2}/[Pu(VII)O_4(OH)_2]^{-3}$ and $[Pu(VIII)O_5OH]^{-3}/Pu(VII)O_5OH]^{-4}$ redox couples, respectively. He concluded that the Pu(VIII/VII) reduction could occur only in extremely high pH alkaline solutions, where the reaction would involve pentaoxo/hydroxo anions. Our calculations for both couples differ by +0.5 V from these results as we predict more positive results with our approach.

All calculated potentials for the Am(VIII/VII) redox couple fall outside the stability range of the water. As predicted for Pu, the most favorable process corresponds to the $[Am(VIII)O_5OH]^{-3}$/$[Am(VII)O_4(OH)_2]^{-3}$ couple with a predicted potential of ∼1.6 V. The predicted potential for the $[Am(VIII)O_4(OH)_2]^{-2}$/$[Am(VII)O_4(OH)_2]^{-3}$ redox couple is approximately the same value. These calculated couples are close to the lower limit estimated by Shilov and Yusov.[38] However, the couple involving pentaoxo/hydroxo complexes had a predicted lower potential of 0.7−0.8 V, differing from those of the other couples. If the same trend holds for Am(VIII), then it is very unlikely that the pentaoxo/hydroxo complex would form under 1 M NaOH (pH = 14) conditions.

An(VII/VI) Redox Potentials. Previous work[20] indicated that the An(VI) species preserve CN = 6 and generate an actinyl dication with 4 OH^- groups in the equatorial region, $[An(VI)O_2(OH)_4]^{-2}$. However, Perethrukhin et al.[9] also suggested the possible formation of $[An(VI)O_2(OH)_3]^{-1}$ and neutral $An(VI)O_2(OH)_2$. Gaona et al.[80] also suggested the presence of $[Np(VI)O_2(OH)_3]^{-1}$ anions at pH 14. Other studies have also suggested the existence of $[UO_2(OH)_5]^{-3}$ in alkaline solutions.[68] However, these species were characterized in highly alkaline media (with TMAOH concentrations of 3.5 or higher). Under the conditions assumed in our work (1 M OH^-), it is unlikely that such species would exist, so we did not consider $[An(VI)O_2(OH)_5]^{-3}$ in our calculations. The An(VII/VI) redox couple reaction explicitly involves H_2O and OH^- molecules, maintaining the octahedral structural arrangement between the hexavalent and heptavalent species. Multiple pathways were evaluated, exploring multiple possibilities for An(VI) (Table 4). For Np(VII/VI), all three +VI species of the dianion, anion, and neutral are consistent with the experimental value of 0.582 V,[32] and, thus, comparison with experiment cannot be used to obtain the speciation. For Pu(VII/VI), the calculated potential using COSMO for formation of the neutral $Pu(VI)O_2(OH)_2(H_2O)_2(H_2O)_{30}$ is in excellent agreement with the experimental value of 0.849 V.[33] The Am(VII/VI) calculated potentials are 1.88 and 2.04 V, with COSMO and SMD, respectively, which are much higher than the estimated value of 1.05 V.[25] This value was estimated based on spectrophotometric data using a linear relationship between the formal redox potentials of hexavalent and heptavalent actinides in alkaline solutions and the energies of the absorption bands associated with charge transfer in their electronic spectra. In general, the calculated potentials are most positive for formation of the dianion $[Np(VI)O_2(OH)_4(H_2O)_{30}]^{-2}$ and least positive for the neutral, but the differences in the potentials of all three species are within 0.2 V making it difficult to assign the speciation by comparing to experiment given the error bars in the calculations and the errors in the experimental estimates.

An(VI/V) Redox Potentials. Although An(V) species have been reported in alkaline solutions, their predominant form has not yet been established. Perethrukhin et al.[9] reported that multiple species are possible, ranging from $AnO_2(OH)$ solids to ionic complexes with a core actinyl group, including $[An(V)O_2(OH)_4]^{-3}$, $[An(V)O_2(OH)_3H_2O]^{-2}$, and $[An(V)O_2(OH)_2(H_2O)_2]^{-1}$. Shilov and Yusov[12] measured the formal potentials of the Np(VI)/Np(V) couple in multiple MOH solutions, with M = Li^+, Na^+, K^+, Cs^+, and $N(CH_3)_4^+$ using potentiometry. They concluded that $[Np(V)O_2(OH)_2]^{-1}$ exists in $[OH^-] \leq 1.0$ M, whereas in more alkaline conditions, the $[Np(V)O_2(OH)_3]^{-2}$ complex is formed. Gelis et al.[35] investigated the redox behavior of Np(VII/VI/V) in

5. An(VI/V) Potentials E^o for Actinides in Alkaline Aqueous Solution Calculated at the B3LYP/ECP(60)/Modified-Level[a]

An(ox)	An(red)	E^o COSMO	E^o SMD	E_{oest}	E_{oexp}
$[U(VI)O_2(OH)_4(H_2O)_{30}]^{-2}$	$[U(V)O_2(OH)_4(H_2O)_{30}]^{-3}$	−0.77	−0.60	−0.69 ± 0.24[26]	−0.65[30]
$[U(VI)O_2(OH)_4(H_2O)_{30}]^{-2}$	$[U(V)O_2(OH)_3(H_2O)(H_2O)_{30}]^{-2}$	−0.56	−0.47		
$[U(VI)O_2(OH)_4(H_2O)_{30}]^{-2}$	$[U(V)O_2(OH)_2(H_2O)_2(H_2O)_{30}]^{-1}$	−0.77	−0.63		
$[U(VI)O_2(OH)_4(H_2O)_{30}]^{-2}$	$U(V)O_2(OH)(H_2O)_3(H_2O)_{30}$	−0.83	−0.65		
$[U(VI)O_2(OH)_3(H_2O)(H_2O)_{30}]^{-1}$	$[U(V)O_2(OH)_4(H_2O)_{30}]^{-3}$	−0.44	−0.39		
$[U(VI)O_2(OH)_3(H_2O)(H_2O)_{30}]^{-1}$	$[U(V)O_2(OH)_3(H_2O)(H_2O)_{30}]^{-2}$	−0.23	−0.26		
$[U(VI)O_2(OH)_3(H_2O)(H_2O)_{30}]^{-1}$	$[U(V)O_2(OH)_2(H_2O)_2(H_2O)_{30}]^{-1}$	−0.44	−0.41		
$[U(VI)O_2(OH)_3(H_2O)(H_2O)_{30}]^{-1}$	$U(V)O_2(OH)(H_2O)_3(H_2O)_{30}$	−0.50	−0.44		
$U(VI)O_2(OH)_2(H_2O)_2(H_2O)_{30}$	$[U(V)O_2(OH)_4(H_2O)_{30}]^{-3}$	−0.21	−0.19		
$U(VI)O_2(OH)_2(H_2O)_2(H_2O)_{30}$	$[U(V)O_2(OH)_3(H_2O)(H_2O)_{30}]^{-2}$	0.00	−0.06		
$U(VI)O_2(OH)_2(H_2O)_2(H_2O)_{30}$	$[U(V)O_2(OH)_2(H_2O)_2(H_2O)_{30}]^{-1}$	−0.21	−0.22		
$U(VI)O_2(OH)_2(H_2O)_2(H_2O)_{30}$	$U(V)O_2(OH)(H_2O)_3(H_2O)_{30}$	−0.27	−0.24		
$[Np(VI)O_2(OH)_4(H_2O)_{30}]^{-2}$	$[Np(V)O_2(OH)_4(H_2O)_{30}]^{-3}$	0.33	0.42	0.38 ± 0.24[26]	0.12,[12] 0.18,[34] 0.106[35]
$[Np(VI)O_2(OH)_4(H_2O)_{30}]^{-2}$	$[Np(V)O_2(OH)_3(H_2O)(H_2O)_{30}]^{-2}$	0.26	0.39		
$[Np(VI)O_2(OH)_4(H_2O)_{30}]^{-2}$	$[Np(V)O_2(OH)_2(H_2O)_2(H_2O)_{30}]^{-1}$	0.14	0.37		
$[Np(VI)O_2(OH)_4(H_2O)_{30}]^{-2}$	$Np(V)O_2(OH)(H_2O)_3(H_2O)_{30}$	0.22	0.52		
$[Np(VI)O_2(OH)_3(H_2O)(H_2O)_{30}]^{-1}$	$[Np(V)O_2(OH)_4(H_2O)_{30}]^{-3}$	0.35	0.40		
$[Np(VI)O_2(OH)_3(H_2O)(H_2O)_{30}]^{-1}$	$[Np(V)O_2(OH)_3(H_2O)(H_2O)_{30}]^{-2}$	0.28	0.36		
$[Np(VI)O_2(OH)_3(H_2O)(H_2O)_{30}]^{-1}$	$[Np(V)O_2(OH)_2(H_2O)_2(H_2O)_{30}]^{-1}$	0.16	0.35		
$[Np(VI)O_2(OH)_3(H_2O)(H_2O)_{30}]^{-1}$	$Np(V)O_2(OH)(H_2O)_3(H_2O)_{30}$	0.24	0.50		
$Np(VI)O_2(OH)_2(H_2O)_2(H_2O)_{30}$	$[Np(V)O_2(OH)_4(H_2O)_{30}]^{-3}$	0.42	0.37		
$Np(VI)O_2(OH)_2(H_2O)_2(H_2O)_{30}$	$[Np(V)O_2(OH)_3(H_2O)(H_2O)_{30}]^{-2}$	0.35	0.34		
$Np(VI)O_2(OH)_2(H_2O)_2(H_2O)_{30}$	$[Np(V)O_2(OH)_2(H_2O)_2(H_2O)_{30}]^{-1}$	0.24	0.32		
$Np(VI)O_2(OH)_2(H_2O)_2(H_2O)_{30}$	$Np(V)O_2(OH)(H_2O)_3(H_2O)_{30}$	0.32	0.47		
$[Pu(VI)O_2(OH)_4(H_2O)_{30}]^{-2}$	$[Pu(V)O_2(OH)_4(H_2O)_{30}]^{-3}$	0.49	0.47	0.16 ± 0.24[26]	0.23,[36] 0.21[37]
$[Pu(VI)O_2(OH)_4(H_2O)_{30}]^{-2}$	$[Pu(V)O_2(OH)_3(H_2O)(H_2O)_{30}]^{-2}$	0.68	0.66		
$[Pu(VI)O_2(OH)_4(H_2O)_{30}]^{-2}$	$[Pu(V)O_2(OH)_2(H_2O)_2(H_2O)_{30}]^{-1}$	0.64	0.70		
$[Pu(VI)O_2(OH)_4(H_2O)_{30}]^{-2}$	$Pu(V)O_2(OH)(H_2O)_3(H_2O)_{30}$	0.70	0.82		
$[Pu(VI)O_2(OH)_3(H_2O)(H_2O)_{30}]^{-1}$	$[Pu(V)O_2(OH)_4(H_2O)_{30}]^{-3}$	0.55	0.74		

$[Pu(VI)O_2(OH)_3(H_2O)(H_2O)_{30}]^{-1}$	$[Pu(V)O_2(OH)_3(H_2O)(H_2O)_{30}]^{-2}$	0.75	0.93		
$[Pu(VI)O_2(OH)_3(H_2O)(H_2O)_{30}]^{-1}$	$[Pu(V)O_2(OH)_2(H_2O)_2(H_2O)_{30}]^{-1}$	0.71	0.98		
$[Pu(VI)O_2(OH)_3(H_2O)(H_2O)_{30}]^{-1}$	$Pu(V)O_2(OH)(H_2O)_3(H_2O)_{30}$	0.77	1.09		
$Pu(VI)O_2(OH)_2(H_2O)_2(H_2O)_{30}$	$[Pu(V)O_2(OH)_4(H_2O)_{30}]^{-3}$	0.69	0.80		
$Pu(VI)O_2(OH)_2(H_2O)_2(H_2O)_{31}$	$[Pu(V)O_2(OH)_3(H_2O)(H_2O)_{30}]^{-2}$	0.88	0.99		
$Pu(VI)O_2(OH)_2(H_2O)_2(H_2O)_{32}$	$[Pu(V)O_2(OH)_2(H_2O)_2(H_2O)_{30}]^{-1}$	0.84	1.04		
$Pu(VI)O_2(OH)_2(H_2O)_2(H_2O)_{33}$	$Pu(V)O_2(OH)(H_2O)_3(H_2O)_{30}$	0.90	1.16		
$[Am(VI)O_2(OH)_4(H_2O)_{30}]^{-2}$	$[Am(V)O_2(OH)_4(H_2O)_{30}]^{-3}$	0.72	0.81	0.65[27]	0.68[29]
$[Am(VI)O_2(OH)_4(H_2O)_{30}]^{-2}$	$[Am(V)O_2(OH)_3(H_2O)(H_2O)_{30}]^{-2}$	0.96	1.06		
$[Am(VI)O_2(OH)_4(H_2O)_{30}]^{-2}$	$[Am(V)O_2(OH)_2(H_2O)_2(H_2O)_{30}]^{-1}$	0.92	1.11		
$[Am(VI)O_2(OH)_4(H_2O)_{30}]^{-2}$	$Am(V)O_2(OH)(H_2O)_3(H_2O)_{30}$	0.98	1.21		
$[Am(VI)O_2(OH)_3(H_2O)(H_2O)_{30}]^{-1}$	$[Am(V)O_2(OH)_4(H_2O)_{30}]^{-3}$	0.79	0.82		
$[Am(VI)O_2(OH)_3(H_2O)(H_2O)_{30}]^{-1}$	$[Am(V)O_2(OH)_3(H_2O)(H_2O)_{30}]^{-2}$	1.02	1.06		
$[Am(VI)O_2(OH)_3(H_2O)(H_2O)_{30}]^{-1}$	$[Am(V)O_2(OH)_2(H_2O)_2(H_2O)_{30}]^{-1}$	0.99	1.11		
$[Am(VI)O_2(OH)_3(H_2O)(H_2O)_{30}]^{-1}$	$Am(V)O_2(OH)(H_2O)_3(H_2O)_{30}$	1.05	1.22		
$Am(VI)O_2(OH)_2(H_2O)_2(H_2O)_{30}$	$[Am(V)O_2(OH)_4(H_2O)_{30}]^{-3}$	0.89	0.83		
$Am(VI)O_2(OH)_2(H_2O)_2(H_2O)_{30}$	$[Am(V)O_2(OH)_3(H_2O)(H_2O)_{30}]^{-2}$	1.12	1.08		
$Am(VI)O_2(OH)_2(H_2O)_2(H_2O)_{30}$	$[Am(V)O_2(OH)_2(H_2O)_2(H_2O)_{30}]^{-1}$	1.09	1.13		
$Am(VI)O_2(OH)_2(H_2O)_2(H_2O)_{30}$ [a]	$Am(V)O_2(OH)(H_2O)_3(H_2O)_{30}$	1.15	1.23		

[a] Potentials in Volts relative to SHE.

concentrated LiOH, NaOH, and NaOH-Na_2CO_3 solutions using both electrochemical and spectrophotometric techniques. They suggested that in the absence of carbonate, the dioxo/tetrahydroxo form $[An(V)O_2(OH)_4]^{-3}$ is the preferred anion at $[OH^-]$ ∼1 M for Np. Shilov[81] reviewed the available redox data at the time, suggesting potentials and possible pathways for the An(V/IV) couple in 1 M NaOH. He stated that Pu(V) probably exists as $[Pu(V)O_2(OH)_4]^{-3}$ or $[Pu(V)O_2(OH)_3H_2O]^{-2}$ anions.

Multiple pathways were explored for the An(VI/V) redox couple, with the results shown in Table 5. For U(VI/V), many pathways involving the ionic forms had predicted potentials close to the experimental potentials of −0.65 V,[30] and the multiple calculated values differed by not more than ±0.2 V. All couples involving the $[U(VI)O_2(OH)_4]^{-2}$ anions displayed acceptable agreement with experiment. For $[U(VI)O_2(OH)_3(H_2O)]^{-1}$, the $[U(VI)O_2(OH)_3(H_2O)]^{-1}/[U(V)O_2(OH)_4]^{-3}$, $[U(VI)O_2(OH)_3(H_2O)]^{-1}$/[U(V)-

https://doi.org/10.1021/acs.jpca.4c08794
J. Phys. Chem. A 2025, 129, 2521−2536

6. An(V/IV) Potentials E^o for Actinides in Alkaline Aqueous Solution Calculated at the B3LYP/ECP(60)/Modified-Level[b]

An(ox)	An(red)	E^o COSMO	E^o SMD	E_{oest}	E_{oexp}
$[U(V)O_2(OH)_4(H_2O)_{30}]^{-3}$	$U(IV)(OH)_4(H_2O)_2(H_2O)_{30}$	−0.82	−0.79	−1.1,[9] −0.03 ± 0.24[26]	
$[U(V)O_2(OH)_4(H_2O)_{30}]^{-3}$	$[U(IV)(OH)_5(H_2O)(H_2O)_{30}]^{-1}$	−0.76	−0.68		
$[U(V)O_2(OH)_4(H_2O)_{30}]^{-3}$	$[U(IV)(OH)_6(H_2O)_{30}]^{-2}$	−0.30	−0.36		
$[U(V)O_2(OH)_3(H_2O)(H_2O)_{30}]^{-2}$	$U(IV)(OH)_4(H_2O)_2(H_2O)_{30}$	−1.03	−0.92		
$[U(V)O_2(OH)_3(H_2O)(H_2O)_{30}]^{-2}$	$[U(IV)(OH)_5(H_2O)(H_2O)_{30}]^{-1}$	−0.97	−0.81		
$[U(V)O_2(OH)_3(H_2O)(H_2O)_{30}]^{-2}$	$[U(IV)(OH)_6(H_2O)_{30}]^{-2}$	−0.51	−0.49		
$[U(V)O_2(OH)_2(H_2O)_2(H_2O)_{30}]^{-1}$	$U(IV)(OH)_4(H_2O)_2(H_2O)_{30}$	−0.82	−0.77		
$[U(V)O_2(OH)_2(H_2O)_2(H_2O)_{30}]^{-1}$	$[U(IV)(OH)_5(H_2O)(H_2O)_{30}]^{-1}$	−0.76	−0.66		
$[U(V)O_2(OH)_2(H_2O)_2(H_2O)_{30}]^{-1}$	$[U(IV)(OH)_6(H_2O)_{30}]^{-2}$	−0.30	−0.33		
$U(V)O_2(OH)(H_2O)_3(H_2O)_{30}$	$U(IV)(OH)_4(H_2O)_2(H_2O)_{30}$	−0.76	−0.74		
$U(V)O_2(OH)(H_2O)_3(H_2O)_{30}$	$[U(IV)(OH)_5(H_2O)(H_2O)_{30}]^{-1}$	−0.70	−0.63		
$U(V)O_2(OH)(H_2O)_3(H_2O)_{30}$	$[U(IV)(OH)_6(H_2O)_{30}]^{-2}$	−0.24	−0.31		
$[Np(V)O_2(OH)_4(H_2O)_{30}]^{-3}$	$Np(IV)(OH)_4(H_2O)_2(H_2O)_{30}$	−0.33	−0.25	−0.09 ± 0.24,[26] −0.95[27]	−0.15,[35] 0.13[38]
$[Np(V)O_2(OH)_4(H_2O)_{30}]^{-3}$	$[Np(IV)(OH)_5(H_2O)(H_2O)_{30}]^{-1}$	−0.06	0.29		
$[Np(V)O_2(OH)_4(H_2O)_{30}]^{-3}$	$[Np(IV)(OH)_6(H_2O)_{30}]^{-2}$	0.25	0.57		
$[Np(V)O_2(OH)_3(H_2O)(H_2O)_{30}]^{-2}$	$Np(IV)(OH)_4(H_2O)_2(H_2O)_{30}$	−0.25	−0.22		
$[Np(V)O_2(OH)_3(H_2O)(H_2O)_{30}]^{-2}$	$[Np(IV)(OH)_5(H_2O)(H_2O)_{30}]^{-1}$	0.01	0.33		
$[Np(V)O_2(OH)_3(H_2O)(H_2O)_{30}]^{-2}$	$[Np(IV)(OH)_6(H_2O)_{30}]^{-2}$	0.32	0.60		
$[Np(V)O_2(OH)_2(H_2O)_2(H_2O)_{30}]^{-1}$	$Np(IV)(OH)_4(H_2O)_2(H_2O)_{30}$	−0.14	−0.21		
$[Np(V)O_2(OH)_2(H_2O)_2(H_2O)_{30}]^{-1}$	$[Np(IV)(OH)_5(H_2O)(H_2O)_{30}]^{-1}$	0.13	0.34		
$[Np(V)O_2(OH)_2(H_2O)_2(H_2O)_{30}]^{1}$	$[Np(IV)(OH)_6(H_2O)_{30}]^{-2}$	0.43	0.62		
$Np(V)O_2(OH)(H_2O)_3(H_2O)_{30}$	$Np(IV)(OH)_4(H_2O)_2(H_2O)_{30}$	−0.22	−0.36		
$Np(V)O_2(OH)(H_2O)_3(H_2O)_{30}$	$[Np(IV)(OH)_5(H_2O)(H_2O)_{30}]^{-1}$	0.05	0.19		
$Np(V)O_2(OH)(H_2O)_3(H_2O)_{30}$	$[Np(IV)(OH)_6(H_2O)_{30}]^{-2}$	0.35	0.47		
$[Pu(V)O_2(OH)_4(H_2O)_{30}]^{-3}$	$Pu(IV)(OH)_4(H_2O)_2(H_2O)_{30}$	−0.20	0.22	−0.67,[9] 0.52 ± 0.24[26]	−0.75,[37] −0.60[39],[a]
$[Pu(V)O_2(OH)_4(H_2O)_{30}]^{-3}$	$[Pu(IV)(OH)_5(H_2O)(H_2O)_{30}]^{-1}$	0.66	0.95		
$[Pu(V)O_2(OH)_4(H_2O)_{30}]^{-3}$	$[Pu(IV)(OH)_6(H_2O)_{30}]^{-2}$	0.80	1.01		
$[Pu(V)O_2(OH)_3(H_2O)(H_2O)_{30}]^{-2}$	$Pu(IV)(OH)_4(H_2O)_2(H_2O)_{30}$	−0.39	0.03		
$[Pu(V)O_2(OH)_3(H_2O)(H_2O)_{30}]^{-2}$	$[Pu(IV)(OH)_5(H_2O)(H_2O)_{30}]^{-1}$	0.47	0.76		
$[Pu(V)O_2(OH)_3(H_2O)(H_2O)_{30}]^{-2}$	$[Pu(IV)(OH)_6(H_2O)_{30}]^{-2}$	0.61	0.82		
$[Pu(V)O_2(OH)_2(H_2O)_2(H_2O)_{30}]^{-1}$	$Pu(IV)(OH)_4(H_2O)_2(H_2O)_{30}$	−0.35	−0.02		
$[Pu(V)O_2(OH)_2(H_2O)_2(H_2O)_{30}]^{-1}$	$[Pu(IV)(OH)_5(H_2O)(H_2O)_{30}]^{-1}$	0.51	0.71		
$[Pu(V)O_2(OH)_2(H_2O)_2(H_2O)_{30}]^{-1}$	$[Pu(IV)(OH)_6(H_2O)_{30}]^{-2}$	0.65	0.77		
$Pu(V)O_2(OH)(H_2O)_3(H_2O)_{30}$	$Pu(IV)(OH)_4(H_2O)_2(H_2O)_{30}$	−0.41	−0.13		
$Pu(V)O_2(OH)(H_2O)_3(H_2O)_{30}$	$[Pu(IV)(OH)_5(H_2O)(H_2O)_{30}]^{-1}$	0.45	0.60		

$O_2(OH)_2(H_2O)_2]^{-1}$, and $[U(VI)O_2(OH)_3(H_2O)]^{-1}/[U(V)O_2(OH)(H_2O)_3$ redox couples are also in agreement with experiment.[30] All pathways involving neutral $U(VI)O_2(OH)_2(H_2O)_2$ deviated significantly from the literature value.[30]

For Np(VI/V), except for $Np(VI)O_2(OH)_2(H_2O)_2/[Np(V)O_2(OH)_4]^{-3}$, all couples are within an acceptable difference from the experimental data (0.10–0.18 V).[12,34,35] For Pu(VI/V), most of the couples using B3LYP differ significantly from experiment (0.21–0.23 V),[35,36] with only the $[Pu(VI)O_2(OH)_4]^{-2}/[Pu(V)O_2(OH)_4]^{-3}$ couple being within 0.3 V. For Am(VI/V), only the couples involving the $[Am(V)O_2(OH)_4]^{-3}$ anion produced acceptable results, namely, the $[Am(VI)O_2(OH)_4]^{-2}/[Am(V)O_2(OH)_4]^{-3}$, $[Am(VI)O_2(OH)_3(H_2O)]^{-1}/[Am(V)O_2(OH)_4]^{-3}$, and $Am(VI)O_2(OH)_2(H_2O)_2/[Am(V)O_2(OH)_4]^{-3}$ couples. Generally, the pathway involving direct electron transfer between dioxo/tetrahydroxo complexes $[An(VI)O_2(OH)_4]^{-2}/[An(V)$-

https://doi.org/10.1021/acs.jpca.4c08794
J. Phys. Chem. A 2025, 129, 2521–2536

7. An(IV/III) Potentials E^{o} for Actinides in Alkaline Aqueous Solution Calculated at the B3LYP/ECP(60)/ModifiedLevel[a]

An(ox)	An(red)	E^{o} COSMO	E^{o} SMD	E_{oest}	E_{oexp}
$U(IV)(OH)_4(H_2O)_2(H_2O)_{30}$	$U(III)(OH)_3(H_2O)_2(H_2O)_{30}$	−2.35	−2.13	−2.78 ± 0.35,[26] −2.6[30]	
$[U(IV)(OH)_5(H_2O)(H_2O)_{30}]^{-1}$	$U(III)(OH)_3(H_2O)_2(H_2O)_{30}$	−2.41	−2.24		
$[U(IV)(OH)_6(H_2O)_{30}]^{-2}$	$U(III)(OH)_3(H_2O)_2(H_2O)_{30}$	−2.87	−2.56		
$Np(IV)(OH)_4(H_2O)_2(H_2O)_{30}$	$Np(III)(OH)_3(H_2O)_2(H_2O)_{30}$	−1.62	−0.96	−1.88 ± 0.24,[26] −1.8,[27] −1.9[31]	
$[Np(IV)(OH)_5(H_2O)(H_2O)_{30}]^{-1}$	$Np(III)(OH)_3(H_2O)_2(H_2O)_{30}$	−1.89	−1.51		
$[Np(IV)(OH)_6(H_2O)_{30}]^{-2}$	$Np(III)(OH)_3(H_2O)_2(H_2O)_{30}$	−2.20	−1.78		
$Pu(IV)(OH)_4(H_2O)_2(H_2O)_{30}$	$Pu(III)(OH)_3(H_2O)_2(H_2O)_{30}$	−0.52	−0.26	−1.04 ± 0.24,[26] −1.0[31]	−0.95[39]
$[Pu(IV)(OH)_5(H_2O)(H_2O)_{30}]^{-1}$	$Pu(III)(OH)_3(H_2O)_2(H_2O)_{30}$	−1.10	−0.73		
$[Pu(IV)(OH)_6(H_2O)_{30}]^{-2}$	$Pu(III)(OH)_3(H_2O)_2(H_2O)_{30}$	−1.24	−0.78		
$Am(IV)(OH)_4(H_2O)_2(H_2O)_{30}$	$Am(III)(OH)_3(H_2O)_2(H_2O)_{30}$	0.33	0.67	0.27,[9] <0.25,[29] 0.06[31]	
$[Am(IV)(OH)_5(H_2O)(H_2O)_{30}]^{-1}$	$Am(III)(OH)_3(H_2O)_2(H_2O)_{30}$	−0.14	0.23		
$[Am(IV)(OH)_6(H_2O)_{30}]^{-2}$	$Am(III)(OH)_3(H_2O)_2(H_2O)_{30}$	−0.17	0.31		

[a] Potentials in volts relative to SHE.

Table 8. Reduction Potentials E^{o} for Pu in Alkaline Aqueous Solution Calculated at PW91/ECP(60)/Modified-TZVP[b]

An(ox)	An(red)	E^{o} COSMO	E^{o} SMD	E_{oest}	E_{oexp}
	VII/VII				
$[Pu(VIII)O_4(OH)_2(H_2O)_{30}]^{-2}$	$[Pu(VII)O_4(OH)_2(H_2O)_{30}]^{-3}$	1.28	1.28	≥1.15[23]	
$[Pu(VIII)O_5(OH)(H_2O)_{30}]^{-3}$	$[Pu(VII)O_5(OH)(H_2O)_{30}]^{-4}$	0.85	0.88		
$[Pu(VIII)O_5(OH)(H_2O)_{30}]^{-3}$	$[Pu(VII)O_4(OH)_2(H_2O)_{30}]^{-3}$	1.64	1.64		
	VII/VI				
$[Pu(VII)O_4(OH)_2(H_2O)_{30}]^{-3}$	$[Pu(VI)O_2(OH)_4(H_2O)_{30}]^{-2}$	0.18	0.39	0.685[14]	0.849[33]
$[Pu(VII)O_4(OH)_2(H_2O)_{30}]^{-3}$	$[Pu(VI)O_2(OH)_3(H_2O)(H_2O)_{30}]^{-1}$	0.15	0.37		
$[Pu(VII)O_4(OH)_2(H_2O)_{30}]^{-3}$	$Pu(VI)O_2(OH)_2(H_2O)_2(H_2O)_{30}$	−0.31	−0.01		
	VI/V				
$[Pu(VI)O_2(OH)_4(H_2O)_{30}]^{-2}$	$[Pu(V)O_2(OH)_4(H_2O)_{30}]^{-3}$	0.36	0.31	0.16[26]	0.23,[36] 0.21[37]
$[Pu(VI)O_2(OH)_4(H_2O)_{30}]^{-2}$	$[Pu(V)O_2(OH)_3(H_2O)(H_2O)_{30}]^{-2}$	0.15	0.16		
$[Pu(VI)O_2(OH)_4(H_2O)_{30}]^{-2}$	$[Pu(V)O_2(OH)_2(H_2O)_2(H_2O)_{30}]^{-1}$	−0.09	0.00		
$[Pu(VI)O_2(OH)_4(H_2O)_{30}]^{-2}$	$Pu(V)O_2(OH)(H_2O)_3(H_2O)_{30}$	0.16	0.26		
$[Pu(VI)O_2(OH)_3(H_2O)(H_2O)_{30}]^{-1}$	$[Pu(V)O_2(OH)_4(H_2O)_{30}]^{-3}$	0.38	0.34		
$[Pu(VI)O_2(OH)_3(H_2O)(H_2O)_{30}]^{-1}$	$[Pu(V)O_2(OH)_3(H_2O)(H_2O)_{30}]^{-2}$	0.17	0.19		
$[Pu(VI)O_2(OH)_3(H_2O)(H_2O)_{30}]^{-1}$	$[Pu(V)O_2(OH)_2(H_2O)_2(H_2O)_{30}]^{-1}$	−0.06	0.02		
$[Pu(VI)O_2(OH)_3(H_2O)(H_2O)_{30}]^{-1}$	$Pu(V)O_2(OH)(H_2O)_3(H_2O)_{30}$	0.19	0.28		
$Pu(VI)O_2(OH)_2(H_2O)_2(H_2O)_{30}$	$[Pu(V)O_2(OH)_4(H_2O)_{30}]^{-3}$	0.84	0.71		
$Pu(VI)O_2(OH)_2(H_2O)_2(H_2O)_{30}$	$[Pu(V)O_2(OH)_3(H_2O)(H_2O)_{30}]^{-2}$	0.63	0.56		
$Pu(VI)O_2(OH)_2(H_2O)_2(H_2O)_{30}$	$[Pu(V)O_2(OH)_2(H_2O)_2(H_2O)_{30}]^{-1}$	0.39	0.40		
$Pu(VI)O_2(OH)_2(H_2O)_2(H_2O)_{30}$	$Pu(V)O_2(OH)(H_2O)_3(H_2O)_{30}$	0.65	0.65		
	V/IV				
$[Pu(V)O_2(OH)_4(H_2O)_{30}]^{-3}$	$Pu(IV)(OH)_4(H_2O)_2(H_2O)_{30}$	−1.03	−0.71	−0.67,[9] 0.52[26]	−0.75,[37] −0.60[39,a]
$[Pu(V)O_2(OH)_4(H_2O)_{30}]^{-3}$	$[Pu(IV)(OH)_5(H_2O)(H_2O)_{30}]^{-1}$	−0.52	−0.27		
$[Pu(V)O_2(OH)_4(H_2O)_{30}]^{-3}$	$[Pu(IV)(OH)_6(H_2O)_{30}]^{-2}$	−0.29	−0.16		
$[Pu(V)O_2(OH)_3(H_2O)(H_2O)_{30}]^{-2}$	$Pu(IV)(OH)_4(H_2O)_2(H_2O)_{30}$	−0.81	−0.56		

$O_2(OH)_4]^{-3}$ provided potentials closest to the experimental values,[12,29,30,34–37] no matter the actinide.

An(V/IV) Redox Potentials. In alkaline media, unlike other redox couples, the An(V/IV) redox potentials reported in the literature exhibit significant variability. The +IV species tend to prefer insoluble forms, amorphous $An(IV)(OH)_4$ or hydrous oxide $An(IV)O_2 \cdot xH_2O$ solids.[82] The structure of the An(IV) neutral hydroxides in an aqueous solution has not been determined experimentally. However, computational studies have provided valuable insights into the structure of An(IV)

https://doi.org/10.1021/acs.jpca.4c08794
J. Phys. Chem. A 2025, 129, 2521–2536

hydroxides in solution. Johnson et al.[83] performed AIMD simulations of a $U(OH)_4$ within a cluster containing 64 H_2O molecules. They predicted that the $U(OH)_4$ species adopts a distorted octahedral structure with two aqua ligands in a cis conformation, *cis*-$U(OH)_4(H_2O)_2$. Huang et al.[84] studied the energetics of $Pu(OH)_4$ and $Pu(OH)_4(H_2O)_n$ clusters with a variety of electronic structure methods including DFT and MP2. The ground state of the $Pu(OH)_4$ species was predicted to have T_d symmetry, and a similar tetrahedral geometry[85] was identified as the ground state for $U(OH)_4$. Huang et al.[84] reported that upon solvation, the structure shifts to a quasisquare-planar $Pu(OH)_4$ geometry, with three H_2O molecules also coordinated to the metal center. To further investigate the structural preferences of An(IV)$(OH)_4$ solvated clusters, we optimized both cis and trans conformations for the neutral hydroxides. Starting from the structure proposed by Huang et al.,[84] the optimization at the B3LYP/ECP(60)/ModifiedTZVP level consistently converged to a minimum geometry where two water molecules were coordinated to the An(IV)$(OH)_4$ clusters. The four hydroxyl groups are positioned in the equatorial plane, and the two water molecules occupy the axial positions, resulting in an octahedral structure denoted as *trans*$U(OH)_4(H_2O)_2$. The *trans*-$U(OH)_4(H_2O)_2$ is always more stable than *cis*-$U(OH)_4(H_2O)_2$, at the B3LYP/ECP(60)/ Modified-TZVP level, and we verified the *trans*-$An(OH)_4(H_2O)_2$ form to be the preferred form for all actinides studied. Consequently, this structure was used as the basis for predicting all of the redox potentials involving An(IV).

Experimental studies suggest the existence of soluble forms of An(IV), as $[An(IV)(OH)_5]^{-1}$ or $[An(IV)(OH)_6]^{-2}$ anions [86–92] in solution, for U, Np, and Pu. The $[NH_4][Np(OH)_5]$ salt provides further corroboration of the formation of pentahydroxo ions.[93] Allard et al.[26] considered the formation of $[An(IV)(OH)_5]^{-1}$ anions at pH 14. However, this was based on assumptions that the total concentration of the dissolved species at pH 8 could be deduced from the solubility product of the hydroxide. Additionally, the concentrations of all species from pH 0 to 14 were calculated by using the hydrolysis constants available at that time. Still, others excluded the existence of these hydrolyzed anions stating a preference for amorphous hydroxides.[94−98] Some studies predict the existence of U(IV)[99] and Np(IV)[91] pentahydroxo-hydrolyzed complexes in solution, whereas others claim that Pu(IV)[91,92] takes the form of hexahydroxo anions. No data are available on the hydrolytic reactions for Am(IV). Experimental studies only reported the existence of insoluble hydroxides, Am(IV)$(OH)_4$ and Am(III)$(OH)_3$ at [NaOH] = 1 M.[100,101] Shilov and Nikolaevskii[102] based on an estimate for the formal potential of the Am(IV)/Am(III) redox couple at 25°C,suggested that $[Am(IV)(OH)_5]^{-1}$ can exist in solution.

We calculated multiple An(V/IV) potentials assuming all possibilities for anionic species for the penta- and tetravalent states (Table 6). The redox potentials calculated for U(V/IV) indicate a significant negative potential consistent with experimental predictions[9,26] that support the unfavorability of such a redox process. The calculated values are consistent with the estimate of −1.1 V from Perethrukhin et al.[9] The potentials closest to the experimental estimates were obtained when considering the neutral U(IV)$(OH)_4(H_2O)_2$ species and $[U(IV)(OH)_5(H_2O)]^{-1}$ anions. Calculations involving the $[U(IV)(OH)_6]^{-2}$ anions differ by more than 0.6 V from the estimated values, independent of the implicit solvation model. The calculated potentials that displayed values closest to the estimated value corresponded to the $[U(V)O_2(OH)_3(H_2O)]^{-2}$/U(IV)$(OH)_4(H_2O)_2$ and $[U(V)O_2(OH)_3(H_2O)]^{-2}$/$[U(IV)(OH)_5(H_2O)]^{-1}$ couples.

For Np(V/IV), in polarographic studies, Peretrukhin and Spitsyn[28] estimated a potential for the Np(V/IV) couple of −0.95 V in 1 M NaOH. However, other studies have reported significantly different values. Shilov and Yusov[38] determined a potential of +0.13 V, and more recently, Gelis et al.[35] reported a value of −0.15 V. Our results are in better agreement with the latter experimental study.[35] All calculated potentials involving neutral hydroxides as the An(IV) form, as well as many involving the $[Np(IV)(OH)_5(H_2O)]^{-1}$ anions, are consistent with the experimental value of −0.15 V.[35] Shilov[81] considered that two pathways are possible for Np, $[Np(V)O_2(OH)_3(H_2O)]^{-2}$/$[Np(IV)(OH)_5(H_2O)]^{-1}$ and $[Np(V)O_2(OH)_2(H_2O)_2]^{-1}$/Np(IV)$(OH)_4$. Both calculated redox couples are in agreement with the experimental data,[35,38] with the latter couple providing the closest match to the experimental values.

Many of the calculated values for the Pu(V/IV) potentials give positive redox potentials, which are consistent with the estimate of 0.52 V given by Allard et al.[26] However, these values differ significantly from the negative potentials obtained in other experimental studies.[37,39] Perethrukhin et al.[9] emphasized that the Pu(V/IV) redox couple exhibits extremely negative potentials, consistent with the strong tendency of Pu(V) to disproportionate. Our values only give negative values when neutral Pu(IV)$(OH)_4(H_2O)_2$ is considered as the Pu(IV) species. Acceptable differences for the negative values were obtained for the $[Pu(V)O_2(OH)_2(H_2O)_2]^{-1}$/Pu(IV)$(OH)_4(H_2O)_2$, $[Pu(V)O_2(OH)_3(H_2O)]^{-2}$/Pu(IV)$(OH)_4(H_2O)_2$, and Pu(V)$O_2(OH)(H_2O)_3$/Pu(IV)$(OH)_4(H_2O)_2$ couples with COSMO. However, the other potentials for the Pu(V)/Pu(IV) couple are all positive and consistent with the estimate of Allard et al.[26] Overall, the couples involving the neutral hydroxides as the Pu(IV) structure displayed potentials in agreement with the experimental values between −0.6 and −0.75 V.[37,39] Our

https://doi.org/10.1021/acs.jpca.4c08794
J. Phys. Chem. A 2025, 129, 2521−2536

results suggest that additional experimental work is needed to define the redox potential for Pu(V)/Pu(IV).

None of the Am(V/IV) potentials involving any anionic forms of Am(IV) yielded potentials within the estimated range[29] of 0.25−0.50 V and the experimental value[39] of 0.20 V. The couples that involve the neutral form $Am(IV)(OH)_4(H_2O)_2$ show the best agreement with the experimental values. Particularly, the couples $[Am(V)O_2(OH)_3]^{-2}$/Am(IV)-$(OH)_4(H_2O)_2$ and $[Am(V)O_2(OH)_3]^{-2}$/Am(IV)-$(OH)_4(H_2O)_2$ differed from the upper limit by less than 0.1 V, and the $Am(V)O_2(OH)(H_2O)_3/Am(IV)(OH)_4(H_2O)_2$ couple, with the COSMO model, was the only case in which a value within the estimated range was obtained. These results suggest that the Am(V/IV) reduction process likely involves Am(IV) existing as solid $Am(OH)_4$ hydroxides, which is consistent with the lack of reported anionic species in solution.

An(IV/III) Redox Potentials. U(III) and Np(III) are known to be readily oxidized by water under alkaline conditions. Conversely, Pu(III) and Am(III) are primarily identified in solution as neutral hydroxides with extremely low solubilities.[103] Allard et al.[26] hypothesized that An(III) species assume the form of $An(III)(OH)_4^{-1}$ anions in solution at pH 14, although such ions have not been observed experimentally. In our study, only neutral hydroxides were considered in the prediction of An(IV/III) potentials. The inaccessibility of these oxidation states is reflected in the estimates reported by Allard et al.[26] and Peretrukhin and Spitsyn,[28] where the U(IV/III) couple was estimated to be −2.6 V, and the Np(IV/III) couple −1.8 V, respectively. For all pathways involving the An(IV/III) couples of U and Np (Table 7), our calculations predict extremely negative potentials.

For the $U(IV)(OH)_4(H_2O)_2/U(III)(OH)_3(H_2O)_2$ couple, the COSMO value is just outside of the error bars of one experimental estimate[26] and within 0.25 V of the other.[30] The dianion $[U(IV)(OH)_6(H_2O)_{30}]^{-2}/U(III)(OH)_3(H_2O)_2$ couple provides the best agreement with the experiment estimates.[26,30] For $Np(IV)(OH)_4(H_2O)_2/Np(III)(OH)_3(H_2O)_2$, the COSMO value is in good agreement with the experimental estimates as are the potentials starting from the anion and dianion.[26,27,31] Using the B3LYP functional, our calculations also indicate negative potentials for the Pu(IV/III) couple, and the pathway involving anionic species of Pu(IV) showed the closest agreement with the experimental measurement of −0.95 V.[39] However, with B3LYP, the pathway involving the neutral ligand differed by more than ±0.4 V from the estimates. Shilov[81] proposed a possible couple for Pu(IV/ III), $[Pu(IV)(OH)_5(H_2O)]^{-1}/Pu(III)(OH)_3$ reduction. The use of the PW91 functional (see below) also gives results consistent with the experimental estimates. For the Am(IV/ III) couple, all three calculated potentials using COSMO are consistent with the experimental estimates.[9,29,31] Our results show that pathways involving Am(III) in its anionic forms yield significantly more negative potentials compared with the neutral pathway.

Results Using the PW91 Functional for Pu. Our previous work demonstrated that the PW91 functional can provide satisfactory results for systems involving Pu, especially for the +VI oxidation state.[40] In general, the potentials are more negative (less positive) with PW91 (Table 8) as compared to B3LYP. For Pu(VIII/VII), the results with the PW91 functional for the pentaoxo/hydroxo complexes are not consistent with the estimated lower bound,[23] in contrast to the B3LYP results where all values were consistent with the lower bound. The PW91 functional-predicted values are much less positive than the experimental values[33] for all possible Pu(VII/VI) couples, and the B3LYP values are in better agreement with experiment. With B3LYP for Pu(VI/V), few redox couples have an acceptable difference from experiment.[36,37] In contrast, most of the Pu(VI)/Pu(V) values using PW91 are within 0.2−0.3 V of experiment.[36,37] Only the $[Pu(VI)O_2(OH)_2(H_2O)_2]/[Pu(V)O_2(OH)_4]^{-3}$, $[Pu(VI)O_2(OH)_2(H_2O)_2]/[Pu(V)O_2(OH)_3(H_2O)]^{-2}$, and $[Pu(VI)O_2(OH)_2(H_2O)_2]/[Pu(V)O_2(OH)(H_2O)_3]$ couples with PW91 are not consistent with experiment.[36,37] The Pu(V/ IV) couples calculated with PW91 tend to favor the more negative range of experimental[37,39] and estimated[9] values, whereas most of the B3LYP couples favored the positive estimated value.[26] Finally, for Pu(IV)/Pu(III), the $[Pu(IV)(OH)_5(H_2O)]^{-1}/Pu(III)(OH)_3(H_2O)_2$ couple provides the best agreement with experiment.[39]

Speciation of Actinides in Alkaline Media. On the basis of the agreement between our calculated potentials and the available experimental data, we can suggest possibilities for the preferred speciation of actinides in aqueous alkaline media. Although for some couples, many redox pathways provided potentials close to experiment, analyzing a range of couples allows us to infer the possible speciation for each oxidation state. It is important to note that our calculations assume standard hydroxide concentrations $[OH^-]$ = 1 mol/L (pH = 14), and these conclusions are only valid at this specific pH and at zero ionic strength and infinite dilution.

The agreement of the calculated An(VIII/VII) potentials with estimates for the $[An(VIII)O_5(OH)]^{-3}/[An(VII)O_4(OH)_2]^{-3}$ and $[An(VIII)O_4(OH)_2]^{-2}/[An(VII)O_4(OH)_2]^{-3}$ suggests the possibility of these two species for An(VIII). Although the existence of the +VIII oxidation state has not been established experimentally, it is likely that the $[An(VIII)O_5(OH)]^{-3}$ form would exist only in very high alkaline concentrations. Therefore, at pH 14, if the +VIII state were to exist under such conditions, then $[An(VIII)O_4(OH)_2]^{-2}$ is the likely species consistent with the results of Gogolev et al.[23] The +VII and +VI oxidation states have been reported,[20,70] and the preferred forms have been assumed

https://doi.org/10.1021/acs.jpca.4c08794
J. Phys. Chem. A 2025, 129, 2521−2536

to be $[An(VII)O_4(OH)_2]^{-3}$ and $[An(VI)O_2(OH)_4]^{-2}$, respectively. All calculated An(VII/VI) potentials employing these species are in agreement with experimental data, except for Am, where the results are not consistent with the estimated values. Considering the +VI preferred form ($[An(VI)O_2(OH)_4]^{-2}$) and the An(VI/V) potentials, the only redox couples consistently in agreement with experiment were those involving $[An(V)O_2(OH)_4]^{-3}$, so we suggest that this species could be the dominant pentavalent form. Finally, the An(V/ IV) and An(IV/III) potentials indicate that +IV and +III oxidation states prefer to assume the form of neutral hydroxides, namely, $An(IV)(OH)_4(H_2O)_2$ and $An(III)(OH)_3(H_2O)_2$, respectively. It is important to note that additional experimental measurements are required to assess these speciation assignments.

CONCLUSIONS

The redox potentials for U, Np, Pu, and Am in oxidation states from +III to +VIII in alkaline aqueous solutions were computed by using density functional theory (DFT) with small-core pseudopotentials and the associated basis sets. Various oxo/hydroxo complexes were considered for each oxidation state, allowing for the evaluation of multiple potentials for many one-electron redox pathways. As in our previous work,[40,41] the calculations incorporated a combined explicit/implicit solvent model approach, in which each complex was surrounded by 30 water molecules to represent explicit local solvation. To account for bulk solvent effects, implicit solvation models were applied, employing the selfconsistent reaction field (SCRF) methods COSMO and SMD. The COSMO SCRF model provided better agreement with experiment in general.

Although species with the +VIII oxidation state have not been experimentally confirmed in aqueous solution, the An(VIII/VII) redox couples involving $[An(VIII)O_5(OH)]^{-3}$/$[An(VII)O_4(OH)_2]^{-3}$, or the direct electron transfer between tetraoxo/dihydroxo complexes $[An(VIII)O_4(OH)_2]^{-2}$/$[An(VII)O_4(OH)_2]^{-3}$, provided potentials in better agreement with other estimates.[23,24] For An(VII/VI), all, including those established as preferable based on experimental data, $[An(VII)O_4(OH)_2]^{-3}$/$[An(VI)O_2(OH)_4]^{-2}$, yielded redox potentials closely matching experimental values for Np[32] and Pu.[33] However, for Am, the calculated potentials differed by more than 0.7 V from the estimates.[25] For An(VI/V) couples, different pathways produced results that were in agreement with experimental data[12,29,30,34−37] within 0.2 V, depending on the specific actinide. Notably, all couples consistently showed that the one-electron redox process, $[An(VI)O_2(OH)_4]^{-2}$/ $[An(V)O_2(OH)_4]^{-3}$, was consistent with the experimental data[12,29,30,34−37] for the four actinides. Similarly, for the An(V/ IV) redox couples, different pathways yielded redox potentials with acceptable differences from the experiment, depending on the specific actinide. However, all redox couples involving neutral hydroxides as the +IV form for the actinide complexes, under the assumption that they exist in their soluble forms, agree with the latest experimental data.[37−39] For the An(IV/ III) couples, the calculations were consistent with estimated literature values,[9,26,27,29−31] assuming the soluble hydroxide form, $An(III)(OH)_3(H_2O)_2$.

Even though alkaline systems involve multiple simultaneous redox reactions, high ionic strength, and the formation of solid hydroxides, which can significantly affect redox measurements, our approach was able to predict potentials that, in many cases, differed by less than ±0.2 V from the experiment or other estimated values. This demonstrates that our approach can be effectively utilized to study the behavior of actinides under basic conditions as well as under acidic conditions.[40,41] Collectively, our results underscore the behavior of actinides in alkaline media and provide a comprehensive framework that aligns with most experimental observations, which advances our understanding of actinide chemistry in alkaline conditions and offers insights into the potential stability and reactivity of various species. Although our approach is useful for aiding the determination of actinide speciation in alkaline media when coupled with experiment, further experimental data are needed to confirm the speciation assignments. The presence of multiple redox couples with calculated potentials in agreement with the experimental values complicates the determination of the speciation of these actinide complexes and will also complicate the experimental analysis.

ASSOCIATED CONTENT

* Supporting Information

The Supporting Information is available free of charge at https://pubs.acs.org/doi/10.1021/acs.jpca.4c08794.

Complete references 54 and 79, energies of each actinide cluster in gas and aqueous phases, spin multiplicities of species and gas-phase Gibbs free energies for each redox reaction, modified-TZVP basis set used in the calculations, and optimized geometries in Cartesian (*x*, *y*, *z*) coordinates (PDF)

https://doi.org/10.1021/acs.jpca.4c08794
J. Phys. Chem. A 2025, 129, 2521−2536

AUTHOR INFORMATION

Corresponding Author

David A. Dixon − *Department of Chemistry and Biochemistry, The University of Alabama, Tuscaloosa, Alabama 35487, United States*; orcid.org/0000-0002-9492-0056; Email: dadixon@ua.edu

Author

Felipe R. Dutra − *Instituto de Química, Universidade Estadual de Campinas, Campinas, São Paulo 13083-970, Brazil; Department of Chemistry and Biochemistry, The University of Alabama, Tuscaloosa, Alabama 35487, United States*

Complete contact information is available at: https://pubs.acs.org/10.1021/acs.jpca.4c08794

Notes

The authors declare no competing financial interest.

ACKNOWLEDGMENTS

This work was supported by the U.S. Department of Energy (DOE), Office of Science, Office of Basic Energy Sciences, Heavy Element Chemistry Program at The University of Alabama (D.A.D.) through Grant No. DE-SC0018921. F.R.D. expresses gratitude for the scholarship provided by grant 2023/ 02596-0, São Paulo Research Foundation (FAPESP). D.A.D. thanks the Robert Ramsay Fund at The University of Alabama.

REFERENCES

(1) Greenwood, N. N.; Earnshaw, A. *Chemistry of the Elements* (2nd Ed.) Oxford: Butterworth-Heinemann, 1997; pp 1250−1284.

(2) Nash, K. L.; Gelis, A. V.; Jensen, M. P.; Bond, A. H.; Sullivan, J. C.; Rao, L.; Garnov, A. Actinides in Alkaline Media: Dissolution, Mineral Associations, and Speciation in Hanford Waste Tank Sludge Simulants. *J. Nucl. Sci. Technol.* 2002, *39*, 512−515.

(3) Silva, R. J.; Nitsche, H. Actinide Environmental Chemistry. *Radiochim. Acta* 1995, *70* (71), 377−396.

(4) Boyarintsev, A. V.; Stepanov, S. I.; Kostikova, G. V.; Zhilov, V. I.; Safiulina, A. M.; Tsivadze, A. Y. Separation and Purification of Elements from Alkaline and Carbonate Nuclear Waste Solutions. *Nucl. Eng. Technol.* 2023, *55*, 391−407.

(5) Altmaier, M.; Gaona, X.; Fanghänel, T. Recent Advances in Aqueous Actinide Chemistry and Thermodynamics. *Chem. Rev.* 2013, *113*, 901−943.

(6) King, W. D.; Edwards, T. B.; Hobbs, D. T.; Wilmarth, W. R. Solubility of Uranium and Plutonium in Alkaline Savannah River Site High Level Waste Solutions. *Sep. Sci. Technol.* 2010, *45*, 1793−1800.

(7) Wan, J.; Tokunaga, T. K.; Larsen, J. T.; Serne, R. J. Geochemical Evolution of Highly Alkaline and Saline Tank Waste Plumes during Seepage through Vadose Zone Sediments. *Geochim. Cosmochim. Acta* 2004, *68*, 491−502.

(8) Deng, Y.; Harsh, J. B.; Flury, M.; Young, J. S.; Boyle, J. S. Mineral Formation during Simulated Leaks of Hanford Waste Tanks. *Appl. Geochem.* 2006, *21*, 1392−1409.

(9) Perethrukhin, V. F.; Shilov, V. P.; Pikaev, A. K *Technical Report0817*; Westinghouse Hanford Company: Richland, WA, USA, 1995.

(10) Nash, K. L. *Characterization of Actinides in Simulated Alkaline Tank Waste Sludges and Leachates*; DOE/FG/63757-final; EMSP Project ID number 81940; TRN: US1001446; United States, 2008, https://www.osti.gov/servlets/purl/941420 (accessed 2024−10−30). (11) Edelstein, N. M.; Fuger, J.; Katz, J. J.; Morse, L. R. Summary and Comparison of Properties of the Actinide and Transactinide Elements. In *The Chemistry of the Actinide and Transactinide Elements*; Morss, L. R.; Edelstein, N. M.; Fuger, J. (Eds.), Springer Netherlands: Dordrecht, 2011; pp 1753−1835.

(12) Shilov, V. P.; Yusov, A. B. Potential of the Np(VI)/Np(V) Couple in Solutions of Various Alkalis. *Radiochem.* 2006, *48*, 24−30. (13) Tananaev, I. G.; Nikonov, M. V.; Myasoedov, B. F.; Clark, D. L. Plutonium in Higher Oxidation States in Alkaline Media. *J. Alloys. Compd.* 2007, *444−445*, 668−672.

(14) Nikonov, M. V.; Gogolev, A. V.; Tananaev, I. G.; Myasoedov, B. F. Experimental Data Points to the Existence of Plutonium(VIII) in Alkaline Solutions. *Mendeleev Commun.* 2005, *15*, 50−52.

(15) Nikonov, M. V.; Myasoedov, B. F. A Spectrophotometric Study of the Reduction of Pu(VIII) and Pu(VII) in Alkaline Solutions. *Radiochem.* 2014, *56*, 227−234.

(16) Domanov, V. P.; Buklanov, G. V.; Lobanov, Y. V. Exotic New Oxides of Plutonium Found by Using Gas Thermochromatography. *J. Nucl. Sci. Technol.* 2002, *39*, 579−584.

(17) Domanov, V. P.; Buklanov, G. V.; Lobanov, Y. V. Formation of Unusual U, Pu, and Cf Oxide Species under Conditions of Gas Thermochromatography. *Radiochem.* 2002, *44*, 114−120.

(18) Nikonov, M. V.; Kiselev, Yu. M.; Myasoedov, B. F. Americium Volatility from Ozonized Alkaline Solutions. *Radiochem.* 2014, *56*, 11−18.

(19) Fedosseev, A. M.; Bessonov, A. A.; Shilov, V. P. Is Octavalent Plutonium Really Formed during Oxidation in Alkaline Aqueous Solutions? *Radiochim. Acta* 2022, *110*, 955−959.

(20) Antonio, M. R.; Williams, C. W.; Sullivan, J. A.; Skanthakumar, S.; Hu, Y.-J.; Soderholm, L. Preparation, Stability, and Structural Characterization of Plutonium(VII) in Alkaline Aqueous Solution. *Inorg. Chem.* 2012, *51*, 5274−5281.

(21) Hübener, S.; Taut, S.; Vahle, A.; Bernhard, G.; Fanghänel, T. Thermochromatographic studies of plutonium oxides. *Radiochim. Acta* 2008, *96*, 781−785.

(22) Shilov, V. P.; Yusov, A. B. Redox Reactions of Actinides in Carbonate and Alkaline Solutions. *Russ. Chem. Rev.* 2002, *71*, 465−488.

(23) Gogolev, A. V.; Fedosseev, A. M.; Moisy, P. The influence of felements' oxidizing potential and ion charge on their stability in aqueous alkaline solution. *Radiochim. Acta.* 2012, *100*, 809−812.
(24) Nikolaevskii, V. B.; Shilov, V. P. *Extreme Oxidation States of Americium. Radiochem.* 2013, *55*, 261−263.
(25) Nikolaevskii, V. B.; Shilov, V. P.; Krot, N. N.; Peretrukhin, V. F. Relationship of the Electronic Absorption Spectra of Hexa- and Heptavalent Actinide Elements in an Alkaline Solution to Their Redox Potentials. *Sov. Radiochem. (Engl. Transl.)* 1975, *17* (3), 426−430.
(26) Allard, B.; Kipatsi, H.; Liljenzin, J. O. Expected Species of Uranium, Neptunium and Plutonium in Neutral Aqueous Solutions. *J. Inorg. Nucl. Chem.* 1980, *42*, 1015−1027.
(27) Nikolaevskij, V. B.; Shilov, V. P.; Krot, N. N. Estimation of Oxidation Potential of Americium (6) in Alkali Medium. *Radiokhimiya* 1974, *16* (1), 122−123.
(28) Peretrukhin, V. F.; Spitsyn, V. I. Electrochemical Determination of the Oxidation Potentials and the Thermodynamic Stability of the Valence States of the Transuranium Elements in Aqueous Alkaline Media. *Russ. Chem. Bull.* 1982, *31*, 726−730.
(29) Peretrukhin, V. F.; Nikolaevskij, V. B.; Shilov, V. P. Electrochemical Properties of Americium Hydroxides in Water-Alkali Medium. *Radiokhimiya* 1974, *16*, 833−836.
(30) Musikas, C.; Rousset, G. Valences Superieures de L'uranium et des Elements Transuramens en Milieu Alcalin. Note CEA, No. 1971, *1419*, 431-436.
(31) Bratsch, S. G. Standard Electrode Potentials and Temperature Coefficients in Water at 298.15 K. *J. Phys. Chem. Ref. Data* 1989, *18*, 1−21.
(32) Zielen, A. J.; Cohen, D. The Neptunium(VII)-(VI) Couple in Sodium Hydroxide Solutions. *J. Phys. Chem.* 1970, *74*, 394−405.
(33) Peretrukhin, V. F.; Krot, N. N.; Gel'man, A. D. Formal Potentials of the Couple Np(VII)–Np(VI) And Pu(VII)–Pu(VI) In Aqueous Solutions With A High Concentration Of Alkali. *Sov. Radiochem. (Engl. Transl.)* 1972, *14* (1), 68−72.
(34) Simakin, G. A.; Matyashchuk, I. V.; Vladimirova, N. A. Potential of the Couple Np (VI)−Np (V) in Sodium Hydroxide Solutions. *Sov. Radiochem., (Engl. Transl.)* 1973, *15* (1), 96−103.
(35) Gelis, A. V.; Vanysek, P.; Jensen, M. P.; Nash, K. L. Electrochemical and Spectrophotometric Investigations of Neptunium in Alkaline Media. *Radiochim. Acta* 2001, *89*, 565−571.
(36) Bourges, J. Preparation and Identification of Pentavalent Plutonium in Basic Medium. *Radiochem. Radioanal. Lett.* 1972, *12* (2−3), 111−19.
(37) Peretrukhin, V. F.; Alekseeva, D. P. Polarographic Properties of Higher Oxidation States of Plutonium in Water-Alkali Solutions. *Radiokhimiya* 1974, *16*, 843−849.
(38) Shilov, V. P.; Yusov, A. B. Investigation of Np(6)+Np(4) Reaction in Alkaline Media. *Radiokhimiya* 1997, *39*, 503−505.
(39) Peretrukhin, V. F.; David, F.; Maslennikov, A. Electrochemical Properties and Thermodynamic Stability of Pu and Neighbouring Actinides in the (IV) and (V) Oxidation States in Aqueous Alkaline Media and Radwastes. *Radiochim. Acta* 1994, *65* (3), 161−166.
(40) Dutra, F. R.; Vasiliu, M.; Gomez, A. N.; Xia, D.; Dixon, D. A. Prediction of Redox Potentials for U, Np, Pu, and Am in Aqueous Solution. *J. Phys. Chem. A* 2024, *128*, 5612−5626.
(41) Dutra, F. R.; Romeu, J. G. F.; Dixon, D. A. Prediction of Redox Potentials for Ac, Th, and Pa in Aqueous Solution. *J. Phys. Chem. A* 2024, *128*, 9730−9746.
(42) Marenich, A. V.; Ho, J.; Coote, M. L.; Cramer, C. J.; Truhlar, D. G. Computational Electrochemistry: Prediction of Liquid-Phase Reduction Potentials. *Phys. Chem. Chem. Phys.* 2014, *16*, 15068−15106.
(43) Ben-Naim, A.; Marcus, Y. J. Solvation Thermodynamics of Nonionic Solutes. *Chem. Phys.* 1984, *81*, 2016−2027.
(44) Zhan, C. G.; Dixon, D. A. First-Principles Determination of the Absolute Hydration Free Energy of the Hydroxide Ion. *J. Phys. Chem. A* 2002, *106*, 9737−9744.
(45) Klamt, A.; Schüürmann, G. COSMO: A New Approach to Dielectric Screening in Solvents with Explicit Expressions for the Screening Energy and Its Gradient. *J. Chem. Soc., Perkin Trans. 2* 1993, *5*, 799−805.
(46) Klamt, A. *Quantum Chemistry to Fluid Phase Thermodynamics and Drug Design*; Elsevier: Amsterdam, 2005; pp 11−47.
(47) Marenich, A. V.; Cramer, C. J.; Truhlar, D. G. Universal Solvation Model Based on Solute Electron Density and on a Continuum Model of the Solvent Defined by the Bulk Dielectric Constant and Atomic Surface Tensions. *J. Phys. Chem. B* 2009, *113*, 6378−6396.
(48) Clark, A. E.; Samuels, A.; Wisuri, K.; Landstrom, S.; Saul, T. Sensitivity of Solvation Environment to Oxidation State and Position in the Early Actinide Period. *Inorg. Chem.* 2015, *54*, 6216−6225.
(49) Parmar, P.; Samuels, A.; Clark, A. E. Applications of Polarizable Continuum Models To Determine Accurate Solution-Phase Thermochemical Values Across a Broad Range of Cation Charge − The Case of U(III−VI). *J. Chem. Theory Comput.* 2015, *11*, 55−63.
(50) Parr, R. G.; Yang, W. *Density-Functional Theory of Atoms and Molecules*; Oxford University Press: New York, 1989.
(51) Becke, A. D. Density-functional Thermochemistry. III. The Role of Exact Exchange. *J. Chem. Phys.* 1993, *98*, 5648−5652.
(52) Lee, C.; Yang, W.; Parr, R. G. Development of the ColleSalvetti Correlation-Energy Formula into a Functional of the Electron Density. *Phys. Rev. B* 1988, *37*, 785−789.
(53) Perdew, J. P.; Chevary, J. A.; Vosko, S. H.; Jackson, K. A.; Pederson, M. R.; Singh, D. J.; Fiolhais, C. Atoms, Molecules, Solids, and Surfaces: Applications of the Generalized Gradient Approximation for Exchange and Correlation. *Phys. Rev. B* 1992, *46*, 6671− 6687.
(54) Frisch, M. J.; Trucks, G. W.; Schlegel, H. B.; Scuseria, G. E.; Robb, M. A.; Cheeseman, J. R.; Scalmani, G.; Barone, V.; Petersson, G. A.; Nakatsuji, H.;et al.*Gaussian 16*, Revision A.03, Gaussian, Inc.: Wallingford CT, 2016.
(55) Peterson, K. A. Correlation Consistent Basis Sets for Actinides.
I. The Th and U Atoms. *J. Chem. Phys.* 2015, *142*, No. 074105.
(56) Küchle, W.; Dolg, M.; Stoll, H.; Preuss, H. Energy-Adjusted Pseudopotentials for the Actinides. Parameter sets and Test Calculations for Thorium and Thorium Monoxide. *J. Chem. Phys.* 1994, *100*, 7535−7542.
(57) Cao, X.; Dolg, M. Segmented Contraction Scheme for SmallCore Actinide Pseudopotential Basis sets. *J. Mol. Struc. - THEOCHEM* 2004, *673*, 203−209.

(58) Cao, X.; Dolg, M.; Stoll, H. Valence Basis Sets for Relativistic Energy-Consistent Small-Core Actinide Pseudopotentials. *J. Chem. Phys.* 2003, *118*, 487−496.

(59) Luchini, G.; Alegre-Requena, J. V.; Funes-Ardoiz, I.; Paton, R. S. GoodVibes: Automated Thermochemistry for Heterogeneous Computational Chemistry Data. *F1000Res.* 2020, *9*, 291.

(60) Ribeiro, R. F.; Marenich, A. V.; Cramer, C. J.; Truhlar, D. G. Use of Solution-Phase Vibrational Frequencies in Continuum Models for the Free Energy of Solvation. *J. Phys. Chem. B* 2011, *115*, 14556− 14562.

(61) Cheng, J.; Liu, X.; VandeVondele, J.; Sulpizi, M.; Sprik, M. Redox Potentials and Acidity Constants from Density Functional Theory Based Molecular Dynamics. *Acc. Chem. Res.* 2014, *47*, 3522− 3529.

(62) Liu, X.; Cheng, J.; Sprik, M. Aqueous Transition-Metal Cations as Impurities in a Wide Gap Oxide: The Cu^{2+}/Cu^{+} and Ag^{2+}/Ag^{+} Redox Couples Revisited. *J. Phys. Chem. B* 2015, *119*, 1152−1163.

(63) Mori-Sánchez, P.; Cohen, A. J.; Yang, W. Localization and Delocalization Errors in Density Functional Theory and Implications for Band-Gap Prediction. *Phys. Rev. Lett.* 2008, *100*, No. 146401.

(64) McNeill, A. S.; Dixon, D. A. Energetics of CO_2^{-} in Aqueous Solution. *J. Phys. Chem. A* 2019, *123*, 1243−1259.

(65) McNeill, A. S.; Zhan, C.-G.; Appel, A. M.; Stanbury, D. M.; Dixon, D. A. The H•/H⁻ Redox Couple and Absolute Hydration Energy of H. *J. Phys. Chem. A* 2020, *124*, 6084−6095.

(66) Andress, T. D.; Maxwell, J. W.; McNeill, A. S.; Stanbury, D. M.; Dixon, D. A. Prediction of Aqueous Reduction Potentials of X•, ChH•, and XO• Radicals with X = Halogen and Ch = Chalcogen. *J. Phys. Chem. A* 2023, *127*, 10600−10612.

(67) Andress, T. D.; Stanbury, D. M.; Dixon, D. A. Calculated Aqueous Reduction Potentials of Neutral and Anionic Halogen Diatomic Molecules. *J. Phys. Chem. A* 2024, *128*, 6494−6509.

(68) Clark, D. L.; Conradson, S. D.; Donohoe, R. J.; Keogh, D. W.; Morris, D. E.; Palmer, P. D.; Rogers, R. D.; Tait, C. D. Chemical Speciation of the Uranyl Ion under Highly Alkaline Conditions. Synthesis, Structures, and Oxo Ligand Exchange Dynamics. *Inorg. Chem.* 1999, *38*, 1456−1466.

(69) Williams, C. W.; Blaudeau, J.-P.; Sullivan, J. C.; Antonio, M. R.; Bursten, B.; Soderholm, L. The Coordination Geometry of Np(VII) in Alkaline Solution. *J. Am. Chem. Soc.* 2001, *123*, 4346−4347.

(70) Bolvin, H.; Wahlgren, U.; Moll, H.; Reich, T.; Geipel, G.; Fanghänel, T.; Grenthe, I. On the Structure of Np(VI) and Np(VII) Species in Alkaline Solution Studied by EXAFS and Quantum Chemical Methods. *J. Phys. Chem. A* 2001, *105*, 11441−11445.

(71) Krot, N. N.; Gel'man, A. D.; Zakharova, F. A.; Peretrukhin, V. F.; Pikaev, A. K. On the Problem of Possibility Plutonium (8) Preparation. *Radiokhimiya* 1972, *14* (6), 890−892.

(72) Huang, W.; Xu, W.-H.; Su, J.; Schwarz, W. H. E.; Li, J. Oxidation States, Geometries, and Electronic Structures of Plutonium Tetroxide PuO_4 Isomers: Is Octavalent Pu Viable? *Inorg. Chem.* 2013, *52*, 14237−14245.

(73) Straka, M.; Dyall, K. G.; Pyykkö, P. Ab Initio Study of Bonding Trends for f^0 Actinide Oxyfluoride Species. *Theor. Chem. Acc.* 2001, *106*, 393−403.

(74) Huang, W.; Pyykkö, P.; Li, J. Is Octavalent Pu(VIII) Possible?
Mapping the Plutonium Oxyfluoride Series PuO_nF_{8-2n} (n = 0−4). *Inorg. Chem.* 2015, *54*, 8825−8831.

(75) Wren, J. E. C.; Schreckenbach, G. Neptunium(VII) in HighIonic-Strength Alkaline Solutions $[NpO_2(OH)_4]^{1-}$ or $[NpO_4(OH)_2]^{3-}$? *Can. J. Chem.* 2009, *87*, 1436−1443.

(76) Tananaev, I. G.; Rozov, S. P.; Mironov, V. S. On the Existence Forms of Heptavalent Plutonium in Aqueous Alkaline Solutions. *Radiokhimiya* 1992, *34*, 88−92.

(77) Tsushima, S. Quantum Chemical Calculations of the Redox Potential of the Pu(VII)/Pu(VIII) Couple. *J. Phys. Chem. B* 2008, *112*, 13059−13063.

(78) Malmqvist, P. Å.; Roos, B. O.; Schimmelpfennig, B. The Restricted Active Space (RAS) State Interaction Approach with Spin−Orbit Coupling. *Chem. Phys. Lett.* 2002, *357*, 230−240.

(79) Aquilante, F.; De Vico, L.; Ferré, N.; Ghigo, G.; Malmqvist, P.; Neogrády, P.; Pedersen, T. B.; Pitoňák, M.; Reiher, M.; Roos, B. O.; et al. MOLCAS 7: The Next Generation. *J. Comput. Chem.* 2010, *31*, 224−247.

(80) Gaona, X.; Fellhauer, D.; Altmaier, M. Thermodynamic Description of Np(VI) Solubility, Hydrolysis, and Redox Behavior in Dilute to Concentrated Alkaline NaCl Solutions. *Pure Appl. Chem.* 2013, *85*, 2027−2049.

(81) Shilov, V. P. Probable Forms of Actinides in Alkali Solutions. *Radiochemistry* 1998, *40*, 11−16.

(82) Choppin, G. R.; Wong, P. J. The Chemistry of Actinide Behavior in Marine Systems. *Aquat. Geochem.* 1998, *4*, 77−101.

(83) Johnson, D. F.; Bhaskaran-Nair, K.; Bylaska, E. J.; de Jong, W. A. Thermodynamics of Tetravalent Thorium and Uranium Complexes from First-Principles Calculations. *J. Phys. Chem. A* 2013, *117* (23), 4988−4995.

(84) Huang, P.; Zavarin, M.; Kersting, A. B. Ab Initio Structure and Energetics of $Pu(OH)_4$ and $Pu(OH)_4(H_2O)_n$ Clusters: Comparison between Density Functional and Multi-Reference Theories. *Chem. Phys. Lett.* 2012, *543*, 193−198.

(85) Lontchi, E. M.; Vasiliu, M.; Tatina, L. M.; Caccamo, A. C.; Gomez, A. N.; Gibson, J. K.; Dixon, D. A. Hydrolysis of Small Oxo/Hydroxo Molecules Containing High Oxidation State Actinides (Th, Pa, U, Np, Pu): A Computational Study. *J. Phys. Chem. A* 2021, *125*, 6158−6170.

(86) Gayer, K. H.; Leider, H. The Solubility of Uranium(IV) Hydroxide in Solutions of Sodium Hydroxide and Perchloric Acid At 25 °C. *Can. J. Chem.* 1957, *35*, 5−7.

(87) Galkin, N. P.; Stepanov, M. A. Solubility of Uranium (IV) Hydroxide in Sodium Hydroxide. *Soviet J. Atomic Energy* 1961, *8*, 231−233.

(88) Tremaine, P. R.; Chen, J. D.; Wallace, G. J.; Boivin, W. A. Solubility of Uranium (IV) Oxide in Alkaline Aqueous Solutions to 300°C. *J. Sol. Chem.* 1981, *10*, 221−230.

(89) Fujiwara, K.; Yamana, H.; Fujii, T.; Kawamoto, K.; Sasaki, T.; Moriyama, H. Solubility of Uranium (IV) Hydrous Oxide in High PH Solution under Reducing Condition. *Radiochim. Acta* 2005, *93*, 347− 350.

(90) Rai, D.; Ryan, J. L. Neptunium(IV) Hydrous Oxide Solubility under Reducing and Carbonate Conditions. *Inorg. Chem.* 1985, *24*, 247−251.

(91) Delegard, C. H. *Determination of the Solubility of Np(IV), Pu(III) - (VI),Am(III) - (VI), and Te(IV), (V) Hydroxo Compounds in 0.5 - 14 M NaOH Solutions*; WHC-EP-0897; ON: DE98058672; BR: EW4030000; TRN: 96000784; United States, 1996. DOI: . (accessed 2024−10−30).

(92) Xiong, Y.; Leigh, C. D. *Modeling Actinide Compounds Solubilities In Alkaline To Hyperalkaline Solutions: Part Two*

Solubility Of Pu(IV) Compounds In NaOH Solutions; SAND2014−15760PE; 533484; United States, 2014. https://www.osti.gov/servlets/purl/1496548. (accessed 2024−10−30).

(93) Cousson, A.; Abavli, H.; Nectouv, F.; Jové, J.; Pages̀, M.; Gasperin, M. Les Hydrovydes de Neptunium (IV): Structure Cristalline de $NH_4Np(OH)_5$ et Etude Par Resonance Mössbauer de Np $(OH)_4$. *J. Less Common Metals* 1986, *121*, 405−414.

(94) Ryan, J. L.; Rai, D. The Solubility of Uranium(IV) Hydrous Oxide in Sodium Hydroxide Solutions under Reducing Conditions. *Polyhedron* 1983, *2*, 947−952.

(95) Parks, G. A.; Pohl, D. C. Hydrothermal Solubility of Uraninite. *Geochim. Cosmochim. Acta* 1988, *52*, 863−875.

(96) Neck, V.; Kim, J. I. Solubility and Hydrolysis of Tetravalent Actinides. *Radiochim. Acta* 2001, *89*, 1−16.

(97) Çevirim-Papaioannou, N.; Yalçıntas̗, E.; Gaona, X.; Dardenne, K.; Altmaier, M.; Geckeis, H. Redox Chemistry of Uranium in Reducing, Dilute to Concentrated NaCl Solutions. *Appl. Geochem.* 2018, *98*, 286−300.

(98) Tits, J.; Gaona, X.; Laube, A.; Wieland, E. Influence of the Redox State on the Neptunium Sorption under Alkaline Conditions: Batch Sorption Studies on Titanium Dioxide and Calcium Silicate Hydrates. *Radiochim. Acta* 2014, *102*, 385−400.

(99) Henry, M.; Merceron, T. An Independent Method for Data Selection of Long-Life Radionuclides (Actinides and Fission Products) in the Geosphere. *Radiochim. Acta* 1994, *66*, 57−62.

(100) Nikonov, M. V.; Gogolev, A. V.; Tananaev, I. G.; Myasoedov, B. F.; Clark, D. L. Redox Behavior of Am(IV) and Methods of Its Preparation in Alkaline Media. *Radiochem.* 2005, *47*, 258−262.

(101) Penneman, R. A.; Coleman, J. S.; Keenan, T. K. Alkaline Oxidation of Americium; Preparation and Reactions of Am(IV) Hydroxide. *J. Inorg. Nucl. Chem.* 1961, *17*, 138−145.

(102) Shilov, V. P.; Nikolaevskii, V. B. Am(II-VII) Species in Aqueous Solutions and Mechanisms of Reactions Involving Them. *Radiochem.* 2014, *56*, 339−363.

(103) Wang, P.; Anderko, A.; Kosinski, J. J.; Springer, R. D.; Lencka, M. M. Modeling Speciation and Solubility in Aqueous Systems Containing U(IV, VI), Np(IV, V, VI), Pu(III, IV, V, VI), Am(III), and Cm(III). *J. Sol. Chem.* 2017, *46*, 521−588.

https://doi.org/10.1021/acs.jpca.4c08794
J. Phys. Chem. A 2025, 129, 2521−2536